Cohesive elements with X-FEM

Summary:

This document presents the various cohesive elements available with the finite element method wide (X-FEM). Three types of cohesive laws are available. The law introduced in first is a regularized law, available for the linear elements, function of the jump of displacement only. Following the limits of the latter, two mixed laws were introduced: one for the linear elements, the other for the quadratic elements. A procedure of propagation of cracks with cohesive elements is implemented. It is based on the linear mixed elements.

The cohesive elements are implemented in *Code_Aster* in 2D and 3D. They are usable with two types of discontinuities: emerging interfaces (keyword TYPE_DISCONTINUITE=' INTERFACE' in DEFI_FISS_XFEM) and cracks of the cohesive type (keyword TYPE_DISCONTINUITE=' COHESIF') that one uses for the studies of propagation on unknown way. The cohesive law is defined in STAT_NON_LINE, the resolution is carried out with the order STAT_NON_LINE [U4.51.03]. For a study of propagation on unknown way, the actualization of fissured surface is done by the order PROPA_FISS, and the directional criterion is calculated by the order CALC_G.

Contents

1 Introduction

Among the classical approaches of breaking process, one counts the laws of damage, for which the mechanical loss of behaviour is described by the degradation of the voluminal properties of material, and two approaches which concentrate this degradation on a surface: approach of Griffith [bib1], and models of cohesive zones (CZM). The model of Griffith consists in carrying out a mechanical calculation on a fissured field, the crack being free constraints, and calculating energy sizes (rate of refund of energy G and factors of intensity of the constraints K_I, K_{II}, to see documentations [R7.02.01] and [R7.02.05]) which start the propagation if a size threshold G_c (which is a property material) is reached.

In spite of this simplicity, this method present disadvantages *for certain applications:*

- If the size of the zone of development of the crack becomes comparable to the lengths characteristic of the model (size of the structure, initial length of crack…), the answer of the structure presents a scale effect which the model of Griffith fails to reproduce. It is generally the case of *concretes and of géomatériaux,* as well as *short cracks*.
- The criterion of propagation of Griffith being implicit, it is very difficult to determine the advance of the face as a curve $G=G_c$. As explained by Fries [bib11], of the very empirical explicit criteria must be used in the place.

In the CZM, forces of cohesion $\boldsymbol{t}_c$ are exerted between the lips of the crack. She obey a lenitive relation of the jump of displacement $[\![\boldsymbol{u}]\!]$, so that they are worth 0 when the crack is entirely open (see fig.1-1).

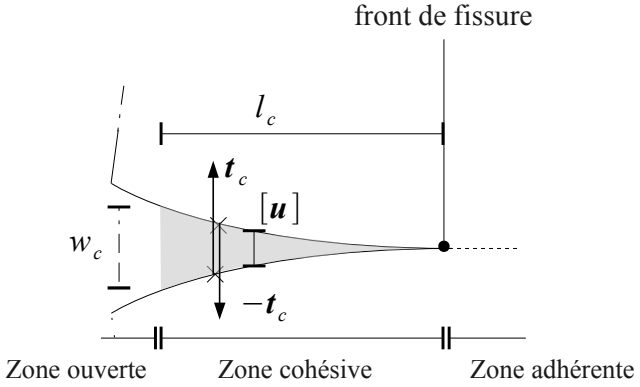

Figure 1-1 : Model of cohesive zone.

In this context, the finite element method wide (XFEM) is a digital technique which makes it possible to insert surfaces of discontinuity through the elements [bib2], and thus to free itself from the constraint to net them. This is particularly useful for studies of propagation of cracks on unknown way: the problems of mending of meshes are avoided.

Three types of cohesive laws are available for elements X-FEM:
– cohesive laws regularized (i.e. with finished initial rigidity) for linear finite elements `CZM_LIN_REG` and `CZM_EXP_REG`. They is the permières introduced laws and simplest, but they present difficulties of convergence since the adherent zone becomes broad.
– mixed cohesive laws (i.e. with infinite initial rigidity) for quadratic finite elements `CZM_OUV_MIX` and `CZM_TAC_MIX`. They more robust and precise, but are reserved for the quadratic elements.

– L has mixed cohesive law CZM_LIN_MIX , for linear finite elements. *The studies of propagation on unknown way are realizable only with the law* CZM_LIN_MIX.

In this document, we start by writing the strong formulation of the problem and by presenting the relations cohesive/jump of displacement for the three cohesive laws forces (cf [§2]). We write then the variational formulation of the problem (cf [§3]). We explain the resolution of the problem by a method of Newton-Raphson (cf [§4]), and present the linearization of the variational formulation. We write the discretization finite elements of the problem, by giving the matric expressions of the tangent matrix and the vectors second member (cf [§5]). Lastly, we detail the procedure of study of propagation of cohesive cracks on unknown way (cf [§6]).

2 Strong formulation of the problem cohesive

2.1 Formulation of the equations of the problem general

Let us note $\Omega \subset \mathbb{R}^d, d \in \{1,2\}$ the field of calculation not fissured. Its border $\partial\Omega$ breaks up into two parts Γ_u and Γ_g, on which displacements and a density of surface efforts are imposed respectively $\boldsymbol{t}$ (see fig.2.1-1). We note Γ *potential zone of cracking* on which is defined the cohesive law, made up of a lip of higher crack Γ^+ and of a lower lip Γ^-. If $\boldsymbol{u^i}$ is displacement on Γ^i, then one introduces the jump of displacement like $[\![\boldsymbol{u}]\!](\boldsymbol{x}) = \boldsymbol{u}^+(\boldsymbol{x}) - \boldsymbol{u}^-(\boldsymbol{x})$. Let us note $\boldsymbol{n}$ the outgoing normal vector of Γ^-, $\boldsymbol{n}^+$ the outgoing normal vector of Γ^+, and $-\boldsymbol{t}_c^+ = \boldsymbol{t}_c^- = \boldsymbol{t}_c$ the force[1] cohesive which applies to Γ^- (see fig.2.1-1). On Γ, we thus have $-\boldsymbol{\sigma}\cdot\boldsymbol{n}^+ = \boldsymbol{\sigma}\cdot\boldsymbol{n} = \boldsymbol{t}_c$. With these conventions, Nous let us have $[\![u_n]\!] = [\![\boldsymbol{u}]\!]\cdot\boldsymbol{n}$ positive in opening and negative in interpenetration (see fig.2.1-1).

Law of behavior	$\boldsymbol{\sigma} = \boldsymbol{C} : \boldsymbol{\varepsilon}$ dans Ω
Balance	$\nabla \cdot \boldsymbol{\sigma} = \boldsymbol{f}$ dans Ω
Imposed surface efforts	$\boldsymbol{\sigma}\cdot\boldsymbol{n}_{ext} = \boldsymbol{t}$ sur Γ_t
Density of the efforts of cohesion	$\boldsymbol{\sigma}\cdot\boldsymbol{n} = \boldsymbol{t}_c$ sur Γ
Imposed displacements	$\boldsymbol{u} = 0$ sur Γ_u

1 Force per unit of area, homogeneous with a constraint

Table 2.1-1 : Equations of the problem general.

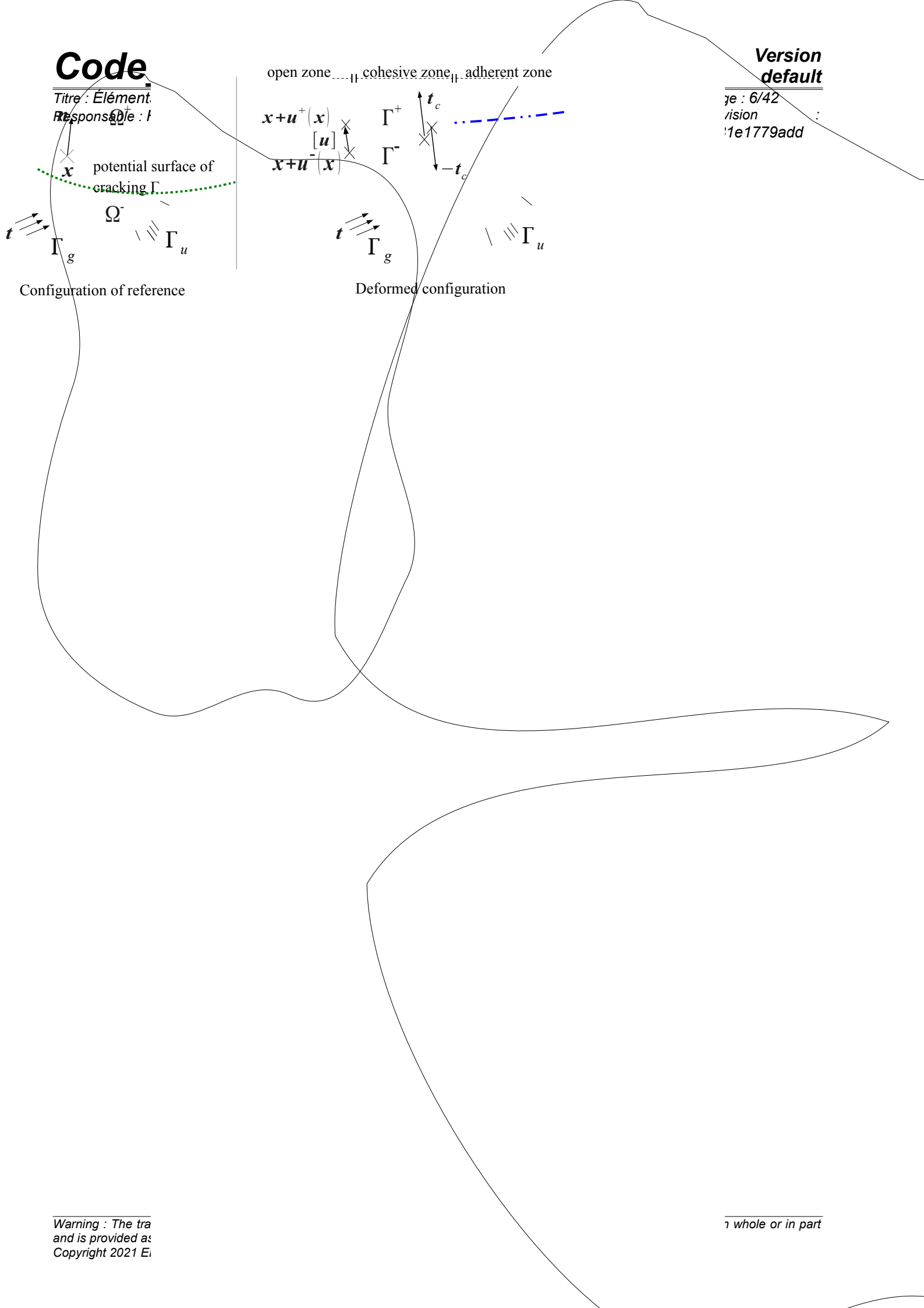

Figure 2.1-1 : Strong formulation of the cohesive problem.

2.2 Cohesive laws

2.2.1 Regularized cohesive laws

The first type of laws which we can consider is a law in which initial adherence is not perfect: the initial slope is finished. Two cohesive laws of this kind are available in Code_Aster, laws CZM_EXP_REG and CZM_LIN_REG whose characteristics are detailed in [R7.02.11]. We recall here of them the principal points, the reader who can refer to it for more details. We detail the extension here to XFEM for the law CZM_EXP_REG, while basing itself on the standard commodity [feeding-bottle 10]. Extension to the law CZM_LIN_REG is made while following the same paradigm exactly.

The opening of a crack in mixed mode is characterized by a criterion of damage defined by means of the jump of equivalent displacement and internal variable α . The material remains in the elastic range as long as the inequality is checked:

$$f(\llbracket u \rrbracket_{eq}, \alpha) = \llbracket u \rrbracket_{eq} - \alpha \leq 0$$

- $\llbracket u \rrbracket_{èq} = \sqrt{\langle \llbracket u_n \rrbracket \rangle_+^2 + \llbracket \boldsymbol{u}_\tau \rrbracket^2}$ is the jump of equivalent displacement,
- $\llbracket \boldsymbol{u}_\tau \rrbracket = \llbracket \boldsymbol{u} \rrbracket - \llbracket u_n \rrbracket \boldsymbol{n}$ is the jump of tangent displacement,
- $\alpha(t) = max\{\alpha_0, \underset{v \in [0,t]}{max} \llbracket u(v) \rrbracket_{éq}\}$ is the internal variable of the cohesive law,
- α_0 is the initial value of α . This value is given by the user via the parameter material PENA_ADHERENCE so that $\alpha_0 = \frac{G_c}{\sigma_c}$ PENA_ADHERENCE .

The cohesive constraint is written then like summons of an elastic constraint, a dissipative constraint and a constraint of penalization which gives an account of the contact:

$$\boldsymbol{t_c} = H\left(\llbracket u \rrbracket_{èq} - \alpha\right) \boldsymbol{\sigma_{lin}} + \left(1 - H\left(\llbracket u \rrbracket_{èq} - \alpha\right)\right) \boldsymbol{\sigma_{dis}} + \boldsymbol{\sigma_{pen}}$$

where H is the indicating function of $\Re^+$

- $\boldsymbol{\sigma}_{pen} = C \langle \llbracket u_n \rrbracket \rangle_- \boldsymbol{n}$ is the constraint of penalization.

where C is a coefficient of penalization clarified in [R7.02.11] given starting from the parameter material PENA_CONTACT.

- $\boldsymbol{\sigma}_{lin} = \boldsymbol{\sigma}_{dis} = \frac{\sigma_c}{\alpha} \exp\left(-\frac{\sigma_c}{G_c} \alpha\right) \llbracket \boldsymbol{u} \rrbracket$ is the expression common to the linear constraints and dissipative, with $\alpha = \llbracket u \rrbracket_{èq}$ for $\boldsymbol{\sigma}_{dis}$.

where σ_c is the critical stress with the rupture and G_c is the energy tenacity of material. It corresponds indeed to energy necessary to the complete opening of the interface over a unit length. A fast calculation with the preceding expressions makes it possible to confirm:

$$\int_{-\infty}^{+\infty} \boldsymbol{t}_{c,\tau} \cdot d[\![\boldsymbol{u}_\tau]\!] + \int_{0}^{+\infty} (\boldsymbol{t}_c \cdot \boldsymbol{n}) d[\![u_n]\!] = G_c$$

One represents on the figure 2.2.1-1 the cohesive constraint for a loading in mode I pure according to the jump of normal displacement.

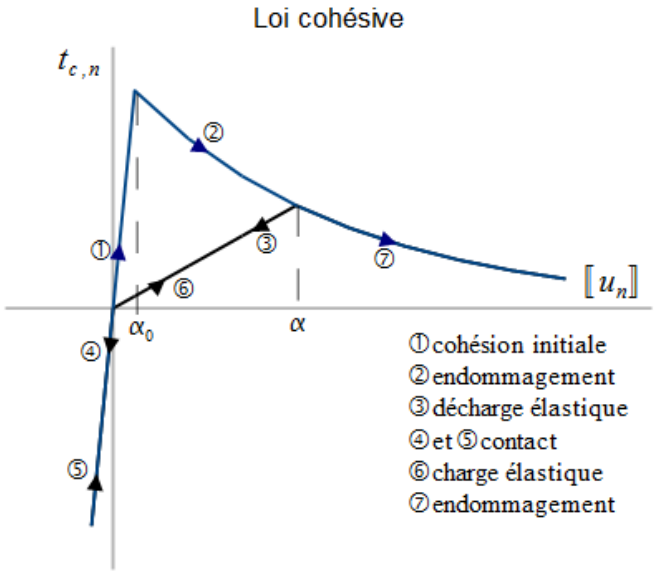

Figure 2.2.1-1: Evolution of the force of normal cohesion according to the jump of displacement.

For $[\![u_n]\!] < 0$, it is also usual to define a force of equivalent cohesion $t_{c,eq}$ thanks to the energy condition of equivalence:

$$t_{c,eq}[\![\dot{u}]\!]_{eq} = t_{c,n}[\![\dot{u}_n]\!] + \boldsymbol{t}_{c,\tau} \cdot [\![\dot{\boldsymbol{u}}_\tau]\!]$$

To find his value, one derives $[\![u]\!]_{èq}$ compared to time.

$$[\![\dot{u}]\!]_{èq} = \frac{[\![\dot{u}_n]\!][\![u_n]\!] + [\![\dot{\boldsymbol{u}}_\tau]\!] \cdot [\![\boldsymbol{u}_\tau]\!]}{[\![u]\!]_{èq}}$$

From where one identifies: $t_{c,èq} = t_{c,n}\frac{[\![u]\!]_{èq}}{[\![u_n]\!]} = \|\boldsymbol{t}_{c,\tau}\|\frac{[\![u]\!]_{èq}}{\|[\![\boldsymbol{u}_\tau]\!]\|} = \frac{\sigma_c}{\alpha}\exp\left(-\frac{\sigma_c}{G_c}\alpha\right)[\![u]\!]_{èq}$

The figure 2.2.1-2 represent the evolution of the force of cohesion equivalent according to the jump of equivalent displacement according to this law of behavior.

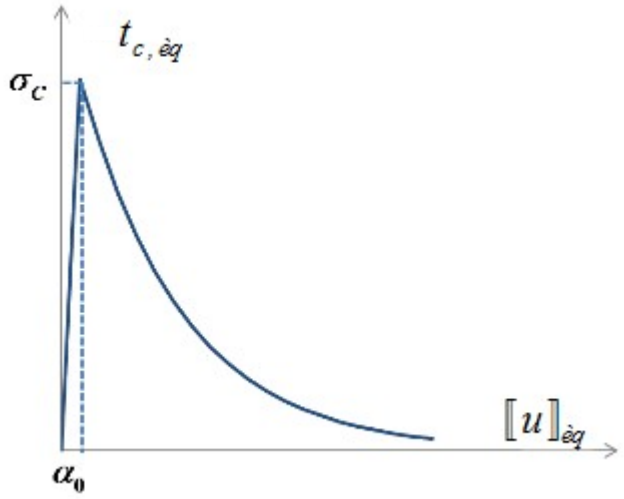

Figure 2.2.1-2: Evolution force of cohesion equivalent according to the jump of displacement are equivalent.

Note:

One defines sometimes a jump of equivalent displacement $[\![u]\!]_{\grave{e}q}=\sqrt{\langle[\![u_n]\!]\rangle_+^2+\beta^2[\![\boldsymbol{u}_\tau]\!]^2}$ *where* β *is an experimental coefficient which represents the report of intensity of the forces of opening in mode* I *and in mode* II*. By taking again the preceding reasoning then with:*

$$t_{c,\grave{e}q}=\frac{\sigma_c}{\alpha}\exp\left(-\frac{\sigma_c}{G_c}\alpha\right)[\![u]\!]_{\grave{e}q}$$

One deduces the expressions from the components:

$$\boldsymbol{t}_{c,n}=\frac{t_{c,eq}[\![u_n]\!]}{[\![u]\!]_{\grave{e}q}}\boldsymbol{n}=\frac{\sigma_c}{\alpha}\exp\left(-\frac{\sigma_c}{G_c}\alpha\right)[\![u_n]\!]\boldsymbol{n}\ ,\ \boldsymbol{t}_{c,\tau}=\beta^2\frac{t_{c,eq}[\![\boldsymbol{u}_\tau]\!]}{[\![u]\!]_{\grave{e}q}}=\beta^2\frac{\sigma_c}{\alpha}\exp\left(-\frac{\sigma_c}{G_c}\alpha\right)[\![\boldsymbol{u}_\tau]\!]$$

2.2.2 Mixed cohesive laws for quadratic elements

The second type of laws which we can consider is, contrary, a law in which initial adherence is perfect: the initial slope is infinite. Two cohesive laws of this kind are available with `XFEM` in Code_Aster, laws `CZM_OUV_MIX` and `CZM_TAC_MIX` whose characteristics are detailed in [R7.02.11]. We recall here the law `CZM_OUV_MIX`, represented on the figure 2.2.2-1.

While noting δ the jump of displacement (this in order to conform to the notations of [R7.02.11]), the material remains in the elastic range as long as:

$$f(\boldsymbol{\delta},\alpha)=\delta_n-\alpha\leq 0$$

On the other hand, this time, the internal variable has a rigorously worthless initial value, so that the constraint is not explicit any more according to displacement, as shown in the figure 2.2.2-1.

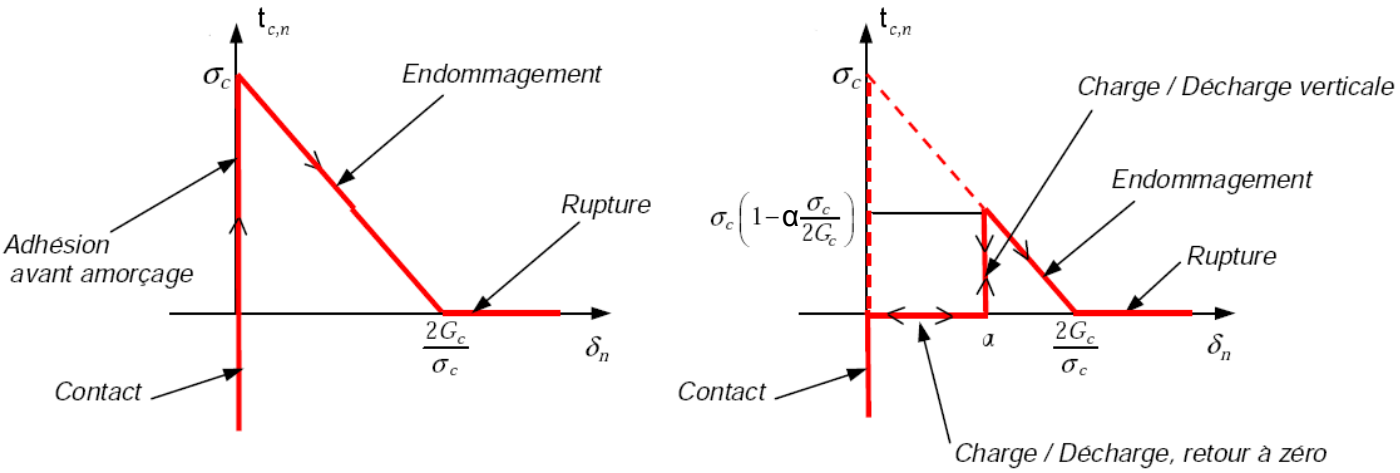

Figure 2.2.2-1: Normal component of the vector forced according to the normal jump for the law CZM_OUV_MIX (threshold α no one on the left and positive on the right).

2.2.3 Mixed cohesive laws for linear elements

The law also has an infinite initial slope, but the discharge is linear (see fig. 2.2.3-1). It is available under the vocabulary CZM_LIN_MIX. To reduce the notations, let us note $\boldsymbol{w}=[\![\boldsymbol{u}]\!]$. In the formalism of Lagrangian increased (see documentations [R5.03.52] and [R5.03.54]), a general expression of the density of energy of surface east:

$$\Pi(\boldsymbol{w},\boldsymbol{\lambda})=\varphi(\boldsymbol{\lambda}+r\boldsymbol{w})-\frac{\boldsymbol{\lambda}\cdot\boldsymbol{\lambda}}{2r}$$

where φ is a derivable function, and r a parameter of increase.

The constraint of interface then is classically given by a derivative compared to the primal variable $\boldsymbol{t}_c=\frac{\partial\Pi}{\partial\boldsymbol{w}}$. One needs an additional equation to determine if one is in the adherent mode, and to impose the corresponding relation of Dirichlet if such is the case. In the formalism of Lagrangian increased, this law of additional interface is determined by derivation compared to the dual variable $\frac{\partial\Pi}{\partial\boldsymbol{\lambda}}=0$. The interest of the method of Lagrangian increased is that there are not other inequalities to check during the resolution: the behavior of interface is entirely contained in these two *equalities*, which allows the use of a method of Newton for the resolution.

The cohesive force is then:

$$\boldsymbol{t}_c(\boldsymbol{\lambda}+r\boldsymbol{w})=\frac{\partial\Pi}{\partial\boldsymbol{w}}=r\frac{\partial\varphi}{\partial(\boldsymbol{\lambda}+r\boldsymbol{w})}$$

The law of interface is written then simply like $\frac{\partial\Pi}{\partial\boldsymbol{\lambda}}=\frac{1}{r}\left[\boldsymbol{t}_c(\boldsymbol{\lambda}+r\boldsymbol{w})-\boldsymbol{\lambda}\right]=0$, which can be rewritten more simply $\boldsymbol{\lambda}=\boldsymbol{t}_c(\boldsymbol{\lambda}+r\boldsymbol{w})$.

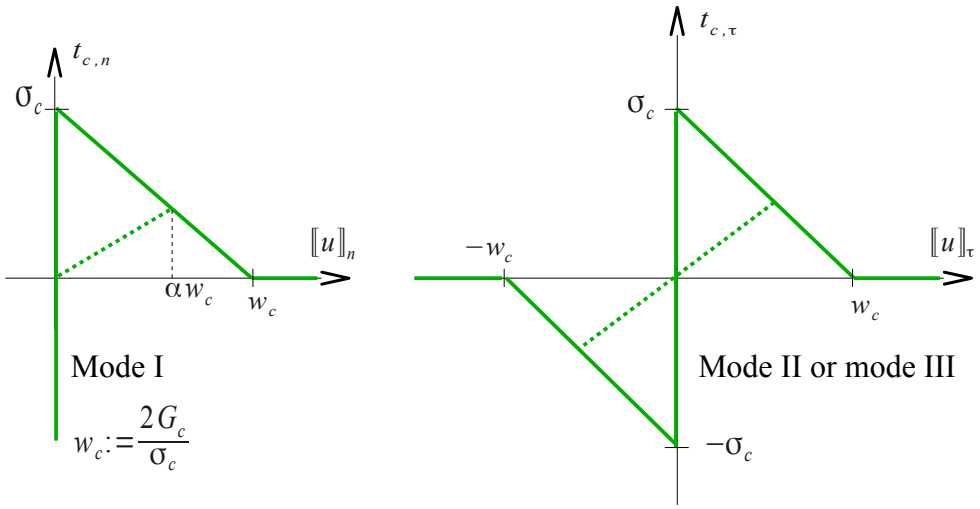

Figure 2.2.3-1 : Mixed cohesive law for linear elements.

An equivalent cohesive force is defined by $(\lambda + r\,w)_{eq} := \sqrt{\langle \lambda_n + r\,w_n \rangle_+^2 + (\boldsymbol{\lambda}_\tau + r\,\boldsymbol{w}_\tau)^2}$. A function threshold ϕ is introduced by $\phi((\lambda + r\,w)_{eq}) := \frac{(\lambda + r\,w)_{eq} - \sigma_c}{r\,w_c - \sigma_c}$. We can then define an internal variable *adimensional* α like maximum of the function threshold in the course of time, projected on the interval $[0,1]$:

$$\tilde{\alpha}(t) = \max_{[0,t]} \phi((\lambda + r\,w)_{eq})$$
$$\alpha = P_{[0,1]}(\tilde{\alpha})$$

The value $\alpha = 0$ (or $\tilde{\alpha} \leq 0$) corresponds to a healthy material (adherent zone), and the value $\alpha = 1$ (or $\tilde{\alpha} \geq 1$) with an entirely fissured material (fissured zone). For conditions of load, i.e. if $\alpha = \phi((\lambda + r\,w)_{eq})$, the function φ is defined by:

$$\varphi(\boldsymbol{\lambda} + r\,\boldsymbol{w}) = 2\,G_c \left(1 - \frac{\sigma_c}{r\,w_c}\right) \alpha \left(1 - \frac{\alpha}{2}\right) + \frac{1}{2r} \langle \lambda_n + r\,w_n \rangle_-^2$$

An expression of the cohesive force $\boldsymbol{t}_c = \frac{\partial \varphi}{\partial \boldsymbol{w}}$ who derives from this energy can then be obtained. By defining an equivalent cohesive force as $t_{c,eq} = \sqrt{\langle t_{c,n} \rangle_+^2 + \boldsymbol{t}_{c,\tau}^2}$, the law forces/opening can be expressed in term of equivalent quantities like $t_{c,eq} = (1 - T_d)(\lambda + r\,w)_{eq}$, where T_d is the function of damage which corresponds to a linear softening:

$$T_d = \frac{\alpha}{\left(1 - \frac{\sigma_c}{w_c r}\right)\alpha + \frac{\sigma_c}{w_c r}}$$

The vectorial relation between cohesive force and jump of displacement is then expressed in terms of normal component $t_{c,n} = (1 - T_d)\langle \lambda_n + r\,w_n \rangle_+ + \langle \lambda_n + r\,w_n \rangle_-$ (the last term having been added to give an account of the unilateral contact) and of tangential component $\boldsymbol{t}_{c,\tau} = (1 - T_d)(\boldsymbol{\lambda}_\tau + r\,\boldsymbol{w}_\tau)$.

3 Variational formulations

Let us transform the strong form of the problem into a weak formulation, adapted better to the finite elements. The field $\boldsymbol{u}$ must belong to the unit V_0 fields of displacements kinematically acceptable:

$$V_0=\left\{ v\in H^1, v \text{ discontinu } à \text{ travers } \Gamma_c, v=0 \text{ sur } \Gamma_u \right\}$$

3.1 Formulation for the regularized cohesive law

We note $H=H^{-1/2}(\Gamma)$ for the cohesive laws. The weak formulation of the cohesive problem is written as follows:
To find $\left(\boldsymbol{u},\boldsymbol{t}_c^+,\boldsymbol{t}_c^-\right)\in V_0\times H\times H$ such as:

$$\int_\Omega \sigma(u):\varepsilon(u^*)\,d\Omega=\int_\Omega f\cdot u^*\,d\Omega+\int_{\Gamma_t} t\cdot u^*\,d\Gamma+\int_{\Gamma^+} t_c^+\cdot u^{*+}\,d\Gamma^+ +\int_{\Gamma^-} t_c^-\cdot u^{*-}\,d\Gamma^- \quad \forall u^*\in V_0$$

Since $[\![\boldsymbol{u}]\!](\boldsymbol{x})=\boldsymbol{u}^+(\boldsymbol{x})-\boldsymbol{u}^-(\boldsymbol{x})$ and $\boldsymbol{t}_c=\boldsymbol{t}_c^-=-\boldsymbol{t}_c^+$, the weak formulation is written in an equivalent way as follows:
To find $u\in V_0$ such as:

$$\int_\Omega \sigma(u):\varepsilon(u^*)\,d\Omega=\int_\Omega f\cdot u^*\,d\Omega+\int_{\Gamma_t} t\cdot u^*\,d\Gamma-\int_{\Gamma_c} t_c\cdot[\![u^*]\!]\,d\Gamma_c \quad \forall u^*\in V_0$$

The current implementation comprises in fact a postprocessing part, in order to give a value to the uncommon multipliers of Lagrange:
To find $\left(u,\lambda_n,\lambda_\tau\right)\in V_0\times H\times H$ such as:
$\forall\left(u^*,\lambda_n^*,\lambda_\tau^*\right)\in V_0\times H\times H$

Equilibrium equation

$$\int_\Omega \sigma(u):\varepsilon(u^*)\,d\Omega-\int_\Omega f\cdot u^*\,d\Omega-\int_{\Gamma_t} t\cdot u^*\,d\Gamma+\int_{\Gamma_c} t_{c,n}\cdot[\![u^*]\!]_n\,d\Gamma_c+\int_{\Gamma_c} t_{c,\tau}\cdot[\![u^*]\!]_\tau\,d\Gamma_c=0$$

Postprocessing left normal

$$\int_{\Gamma c}\left(\lambda_n-t_{c,n}\cdot n\right)\lambda_n^*\,d\Gamma_c=0$$

Postprocessing left tangential

$$\int_{\Gamma c}\left(\lambda_\tau-t_{c,\tau}\right)\lambda_\tau^*\,d\Gamma_c=0$$

Thus, multipliers λ_n and λ_τ do not intervene in the resolution. They are only used to store the cohesive constraints in an explicit way.

3.2 Disadvantages of a regularized cohesive law

In order to evaluate the capacity of such a cohesive law to describe the adherent zone suitably, a test of opening of a circular inclusion is carried out. Geometry and loading are given in figure 3.2-1 (dimensions in millimetres). It is about a plate under tension in plane deformations, with $E=36.56\,GPa$ and $\nu=0.2$. A circular inclusion is inserted in the plate, which is supposed to be able to open according to a cohesive law of critical stress $\sigma_c=2.7\,MPa$, and energy tenacity $G_c=0.095\,N.mm^{-1}$.

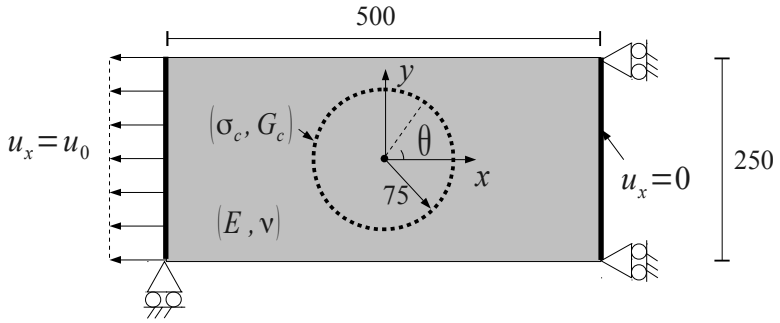

Figure 3.2-1 : Test of opening of a circular inclusion.

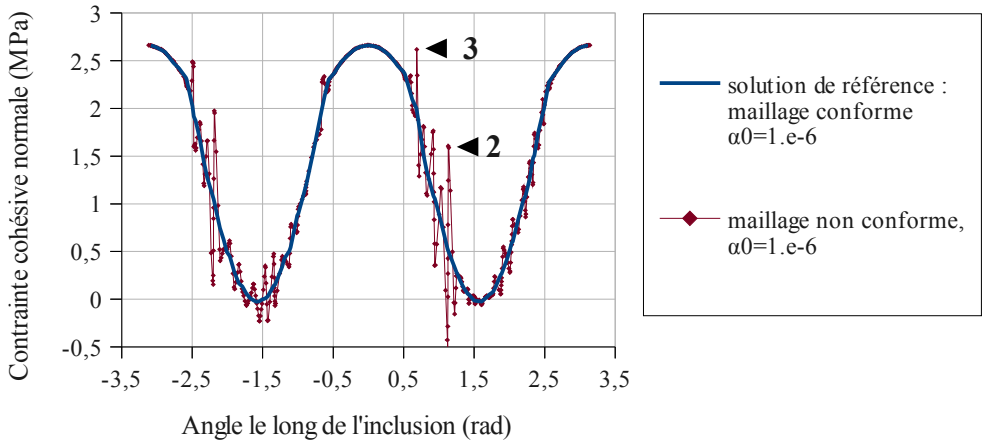

Figure 3.2-2 : Normal cohesive force along inclusion.

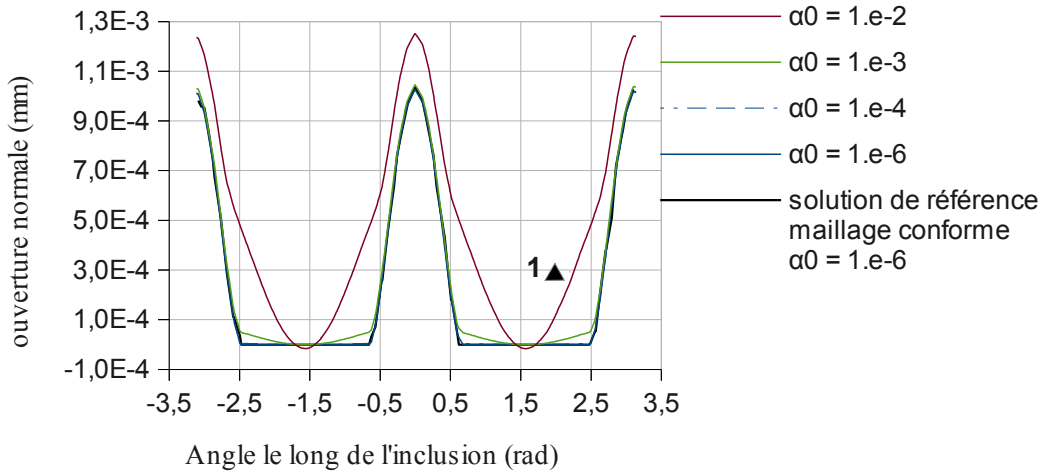

Figure 3.2-3 : Jump of normal displacement along inclusion.

The jump of normal displacement and the force which is deduced from it are traced on the figures 3.2-2 and 3.2-3, for a loading $u_0 = 0.04\ mm$, for grids in conformity or not on the fissured surface, and for

parameters of penalization $\alpha_0=10^{-2}$ and $\alpha_0=10^{-6}$. As we can see it on the figures, the regularized cohesive laws present three difficulties:

1. if the penalization is too weak, the jump of displacement along inclusion is false: one observes an opening which is not physical (mark 1 on the fig.3.2-3);
2. if, on the contrary, the penalization is too high, *parasitic oscillations* cohesive constraint appraissent in the adherent zone (mark 2 on the fig.3.2-2). This problem was abundantly announced in the literature (see for example [bib3]). Originally noticed within the framework of the contact for Code_Aster, and indicated under the term of "condition LBB", it is treated in documentation [R5.03.54], §6. In a word, it comes owing to the fact that the space of discretization of the cohesive forces becomes too rich in comparison with that of displacement, when the stiffness of the law becomes such as one approaches a condition of Dirichlet;
3. *a bad evaluation of the mode of operation* (member or dissipative) can arrive as a consequence of these oscillations (mark 3 on the fig3.2-2).

To conclude, the penalized laws fail to give a faithful representation of the adherent zones, since a parameter of penalization α_0^{-1} too much small implies an opening not-physics of the adherent zone, which leads to a false solution, while a too large parameter α_0^{-1} generate parasitic oscillations because of a problem of stability, since the parameter of penalization starts to become suffisement important to describe adherence suitably.

By considering the test of wrenching of the figure 3.2-4 (this test is digital, it does not correspond to any physical reality), it is possible to highlight in a way even more obvious the phenomenon of oscillations.

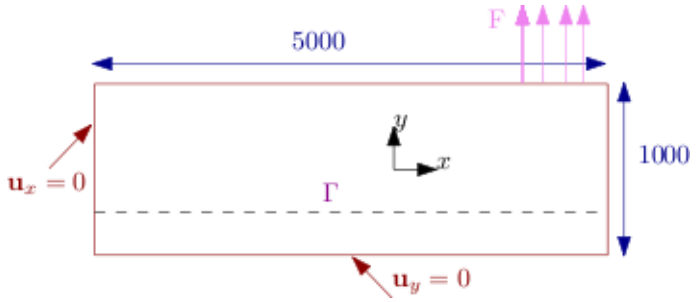

Figure 3.2-4 : Test of wrenching: geometry and loading.

The parameters for this test are the following: $E=30\,GPa$, $\nu=0.2$, $\sigma_c=0.2\,MPa$, $G_c=2\,N.mm^{-1}$ and $\alpha_0=10^{-6}$. We repésenté in figure 3.2-5 the constraint of interface for a grid in conformity, which is used as reference, and the constraint for a grid nonin conformity. The phenomenon of parasitic oscillations of digital origin is particularly visible there on all the adherent zone.

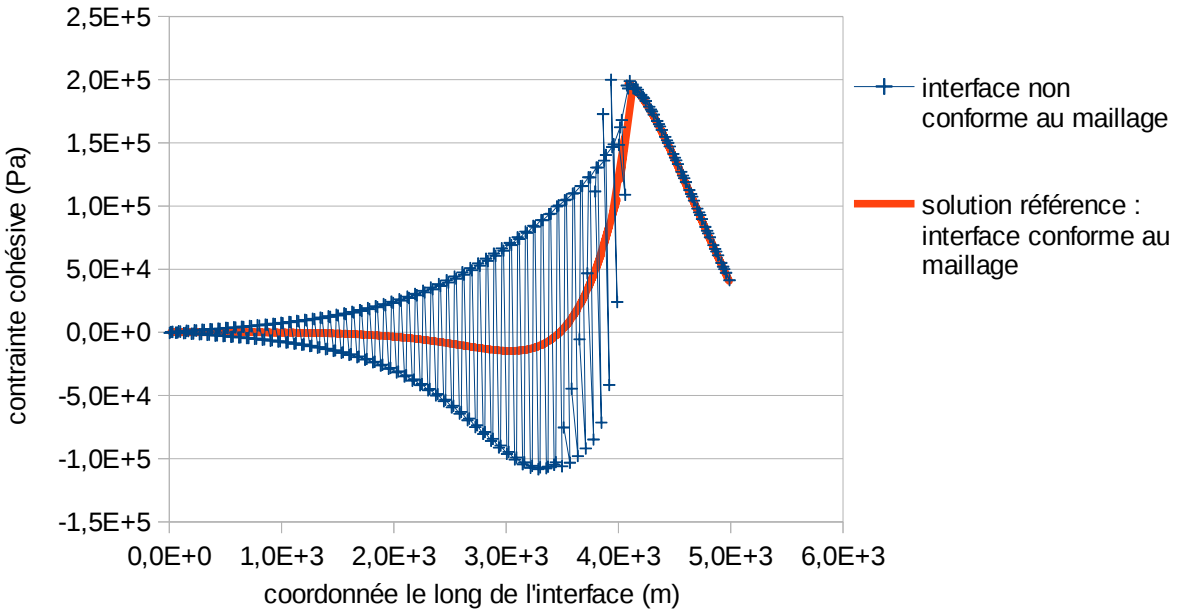

Figure 3.2-5 : Test of wrenching: cohesive constraint along the interface.

3.3 Space reduced for the discretization of the constraint of interface

For a detailed description of the discretization of the unknown factors of contact, the reader can refer to documentation [R5.03.54], §5. In short, them *initial components* multiplier are defined on the nodes tops K elements parents intersected (see fig. 3.3-1). Implementation such elements of contact is detailed in [R5.03.54], §4. One imposes then rekations of equality between some of these *initial components* in order to lead to a lower number N_λ of *degrees of freedom* indeed independent. These relations are carried by certain intersected edges V , known as vital edges: a degree of freedom I really independent is divided by a group of nodes of K (see fig. 3.3-1), which produces a function of wide form of contact $\psi_I := \sum_{i \in I} N_i$ (see fig. 3.3-1). The algorithm of selection of such vital edges, and thus of contruction of reduced space, is detailed in documentation [R5.03.54], §6. The field of multipliers is then obtained by interpolation on the elements parents and the discrete multiplier is the trace of this field on the interface:

$$\boldsymbol{M}_h := \left\{ \sum_I \boldsymbol{\mu}_I \psi_I|_\Gamma , \boldsymbol{\mu}_I \in \mathbb{R}^d \right\}$$

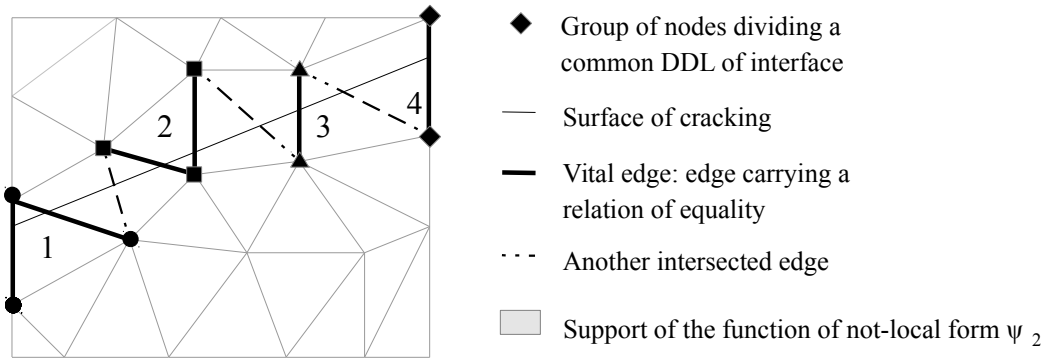

Figure 3.3-1 : Grid nonin conformity with the crack and reduced space of multipliers.

3.4 Formulation for a mixed cohesive law for quadratic elements

By opposition to the preceding formulation, the treatment of such a law will require a true formulation with several fields, in the direction where one vectorial dual field λ goes indeed to enter in the formulation, instead of being an artifice of post - treatment as in §3.1. This formulation follows an energy reasoning, explained in detail in documentation [R3.06.13]. Let us summarize in the principal points:

It is written that the opening of the crack costs an energy proportional to surface to be opened, that is to say :

$$E_{\mathrm{fr}}(\boldsymbol{\delta})=\int_{\Gamma} \Pi(\boldsymbol{\delta})\, dS$$

where $\Pi(\boldsymbol{\delta})$ is the density of cohesive energy. For the law CZM_OUV_MIX , we have for example $\Pi(\boldsymbol{\delta})=\int_0^{\delta_n} t_{c,n}(\delta')\, d\,\delta'$.

The field of discontinuity δ appearing in the preceding expressions is then defined like a field except for whole, integrated in the formulation as a new unknown factor . Total energy is written then:

$$E(\boldsymbol{u},\boldsymbol{\delta})=\int_{\Omega\setminus\Gamma} \Phi(\boldsymbol{\varepsilon}(\boldsymbol{u}))\, d\Omega - W_{ext}(\boldsymbol{u})+\int_{\Gamma} \Pi(\boldsymbol{\delta})\, d\Gamma$$

The solution of the problem consists then of the minimization of this total energy under the constraint that δ corresponds to the jump of displacement. One seeks:

$$\min_{\substack{u,\delta \\ [\![\boldsymbol{u}]\!]=\boldsymbol{\delta}}} E(\boldsymbol{u},\boldsymbol{\delta})$$

In order to solve this one, we introduce the Lagrangian associated one with the problem, to which we add a term of increase whose utility will appear thereafter:

$$L_r(\boldsymbol{u},\boldsymbol{\delta},\boldsymbol{\lambda}) \underset{déf.}{=} E(\boldsymbol{u},\boldsymbol{\delta})+\int_{\Gamma} \boldsymbol{\lambda}\cdot([\![\boldsymbol{u}]\!]-\boldsymbol{\delta})\, d\Gamma+\int_{\Gamma} \frac{r}{2}([\![\boldsymbol{u}]\!]-\boldsymbol{\delta})^2\, d\Gamma$$

We can then write the first condition of optimality of this Lagrangian:

$$\forall\ \delta^* \quad \int_{\Gamma} \left[\boldsymbol{t}_c-\boldsymbol{\lambda}+r\ (\boldsymbol{\delta}-[\![\boldsymbol{u}]\!])\right]\cdot\boldsymbol{\delta}^*=0 \quad \text{avec} \quad \boldsymbol{t}_c\in\partial\,\Pi(\boldsymbol{\delta})$$

This equation fact of intervening the cohesive constraint $\boldsymbol{t}_c$. However we do not have like expression $\boldsymbol{t}_c$ that of a local law of behavior. This first equation thus must, to have direction, to be discretized in

a way which makes it possible to be brought back to a local expression . This is possible if δ is discretized by collocation at the points of Gauss of the interface, coordinates $\boldsymbol{x}_g$.
Indeed, with such a discretization , the resolution of the first condition of optimality come down to satisfy the cohesive law in each point with collocation:

$$t_c\left(\delta_g,\alpha_g\right)=\lambda_g+r\left(\left[\!\left[u_g\right]\!\right]-\delta_g\right)$$

where we noted $\lambda_g=\lambda\left(x_g\right)$, for example, values of a field at the points of Gauss, and where $t_c\left(\delta_g,\alpha_g\right)$ the law follows 2.2.2-1 . The graphic translation of this law of behavior is the following one: the solution corresponds to the intersection of the linear function $\delta\rightarrow\lambda_g+r\left[\!\left[u_g\right]\!\right]-r\ \delta$ (with a negative slope given by the coefficient of penalty r) with the graph $t_c\left(\delta,\alpha\right)$. We see whereas for r rather large, the solution is single, from where interest to have increased the Lagrangian one.

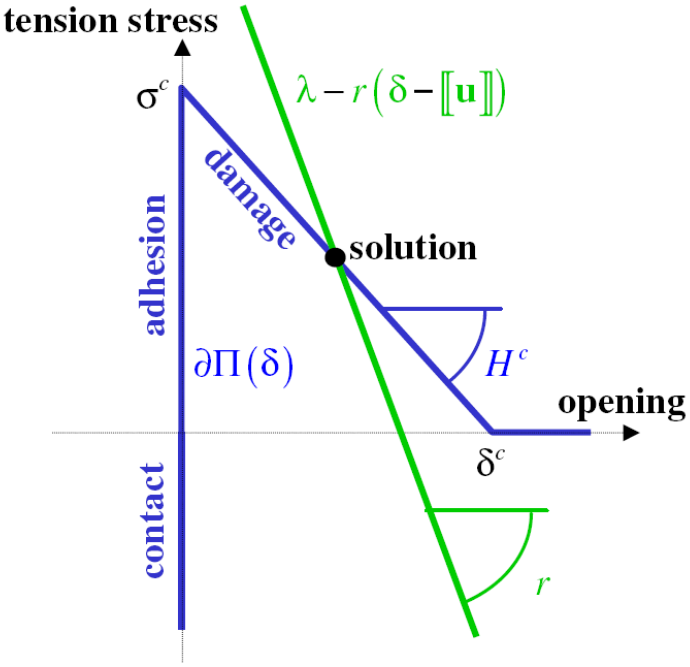

Figure 3.4-a : Solution of the integration of the behavior.

The field δ is thus written locally like a function of $\lambda+r\left[\!\left[u\right]\!\right]$, that we will call increased multiplier and will note p . Consequently, it disappears from the unknown fields of the problem. The formulation is then given by the two conditions of optimality of Lagrangian remaining:
To find $\left(u,\lambda\right)\in V_0\times H$ such as:
$\forall\left(u^*,\lambda^*\right)\in V_0\times H$

Equilibrium equation
$$\int_\Omega\sigma\left(u\right):\varepsilon\left(u^*\right)d\,\Omega-\int_\Omega f\cdot u^*d\,\Omega-\int_{\Gamma_t}t\cdot u^*d\,\Gamma+\int_{\Gamma_c}\left[\lambda+r\left(\left[\!\left[u\right]\!\right]-\delta\left(p\right)\right)\right]\cdot\left[\!\left[u^*\right]\!\right]d\,\Gamma=0\quad\text{avec}\quad p=\lambda+r\left[\!\left[u\right]\!\right]$$

Law of interface
$$\int_{\Gamma_c}\left[\left[\!\left[u\right]\!\right]-\delta\left(p\right)\right]\cdot\lambda^*d\,\Gamma=0$$

With regard to the discretization of these two fields of unknown factors, a simple discretization observing the stability condition inf-sup, and consistent with the discretization of δ by collocation, consists in discretizing it displacement with P2 elements and it multiplier in a way P1 on a reduced space adapted to X-FEM, like detailed in §3.3 or in [R5.03.54], §6 .

3.5 Formulation for a mixed cohesive law for linear elements

As shown before, the quantities with the interface must be defined on a reduced space $\boldsymbol{M}_h$ in order to prevent parasitic oscillations of digital origin in the adherent phases. This applies to the cohesive constraints $\boldsymbol{\lambda}$ and $\boldsymbol{t}_c$. In fact, $\boldsymbol{t}_c$ depends on $\boldsymbol{\lambda}+r\,\boldsymbol{w}$ where $\boldsymbol{w}$ is the jump of displacement. As a consequence of this increase, in particular present at the time of the adherent phases, $\boldsymbol{w}$ must also be written on consistent space $\boldsymbol{M}_h$.

Note:

Another way of being convinced some consists in considering a problem of pure adherence, adherence being described by a regularized law. This problem indeed describes the behavior of the term of increase at the time of the adherent phases. To avoid oscillations, we saw that a penalized law must be suitably written on reduced space, so that the system to be solved is:

$$\begin{bmatrix} K_u^1 & 0 & 0 \\ 0 & K_u^2 & A^T \\ 0 & A & \frac{1}{r}C \end{bmatrix} \begin{Bmatrix} \{a\} \\ \{b\} \\ \{\lambda\} \end{Bmatrix} = \begin{Bmatrix} \{L_{\text{méca}}^1\} \\ \{L_{\text{méca}}^2\} \\ 0 \end{Bmatrix}$$

where:

- *we gather in* $\{L_{\text{méca}}\}$ *and* $[K_u]$ *discretization of all the terms which are not terms of interface;*
- $C_{IK}=\int_\Gamma \psi_I \psi_K d\Gamma$ *;*
- $A_{Ij}=\int_\Gamma \psi_I \varphi_j d\Gamma$ *;*
- $\{a\}$ *is the vector gathering the classical DDL of displacement;*
- $\{b\}$ *that of the DDL nouveau riches;*
- $\{\lambda\}$ *gather DDL of the multiplier to the interface, discretization which is carried out on reduced space* M_h *;*
- r *is the parameter of penalization.*

In a formulation penalized consistent, we can interpret the constraint of interface like proportional to a consistent jump $\{w\}$ *:* $\{\lambda\}=r\{w\}$ *. With the preceding matric expression, we can then identify* $\{w\}=[C]^{-1}[A]\{b\}$ *.*

We could then condense the preceding matric system to eliminate $\{\lambda\}$ *:*
$[K_u^2]\{b\}+[A]^T\{\lambda\}=[K_u^2]\{b\}+[A]^T\left(r[C]^{-1}[A]\{b\}\right)$

We see whereas the resolution would require the assembly and the calculation of a matrix $[A]^T[C]^{-1}[A]$ *.*
Such a matric product is not realizable in an elementary calculation, with stronger reason taking into account the character not-room of $\boldsymbol{M}_h$ *. Such a total operation thus goes against the data-processing architecture of Code_Aster, and must be proscribed as far as possible.*

To avoid the problem, $\boldsymbol{w}$ is introduced like a new unknown factor of the problem, which is not discretized like $[\![\boldsymbol{u}]\!]$ but is a projection on a reduced space $\boldsymbol{M}_h$. Broken up using this field from now on available in the formulation, the preceding term of stabilization could be determined by assembly of an elementary calculation. The total energy of the problem is written:

$$E(\boldsymbol{u},\boldsymbol{\lambda},\boldsymbol{w})=\frac{1}{2}\int_\Omega \epsilon(\boldsymbol{u}):C:\epsilon(\boldsymbol{u})\,d\Omega-\int_{\Gamma_g}\boldsymbol{g}\cdot\boldsymbol{u}\,d\Gamma_g+\int_\Gamma \Pi\left(\boldsymbol{w},\boldsymbol{\lambda}\right)d\Gamma$$

The solution of the continuous problem consists of a minimization under constraints of equality $\left(\boldsymbol{u},\boldsymbol{w},\boldsymbol{\lambda}\right)=\underset{\boldsymbol{w}^{*}=[\![\boldsymbol{u}^{*}]\!]}{argmin}E\left(\boldsymbol{u}^{*},\boldsymbol{\lambda}^{*},\boldsymbol{w}^{*}\right)$. We can write the Lagrangian associated one like:

$$L\ \left(\boldsymbol{u},\boldsymbol{w},\boldsymbol{\lambda},\boldsymbol{\mu}\right)=\frac{1}{2}\int_{\Omega}\epsilon(\boldsymbol{u}):C:\epsilon(\boldsymbol{u})\,d\,\Omega-\int_{\Gamma_{g}}\boldsymbol{g}\cdot\boldsymbol{u}\,d\,\Gamma_{g}+\int_{\Gamma}\Pi(\boldsymbol{w},\boldsymbol{\lambda})\,d\,\Gamma+\int_{\Gamma}\boldsymbol{\mu}\cdot\left([\![\boldsymbol{u}]\!]-\boldsymbol{w}\right)d\,\Gamma$$

The writing of the conditions of optimality of this Lagrangian led to the following variational formulation:

Equilibrium equation $\forall\,\boldsymbol{u}^{*}\in\boldsymbol{V}_{h},\int_{\Omega}\sigma(\boldsymbol{u}):\epsilon(\boldsymbol{u}^{*})\,d\,\Omega-\int_{\Gamma_{g}}\boldsymbol{g}\cdot\boldsymbol{u}^{*}\,d\,\Gamma_{g}+\int_{\Gamma}\boldsymbol{\mu}\cdot[\![\boldsymbol{u}^{*}]\!]\,d\,\Gamma=0$

Projection of the jump of displacement $\forall\boldsymbol{\mu}^{*}\in\boldsymbol{M}_{h},\int_{\Gamma}\left([\![\boldsymbol{u}]\!]-\boldsymbol{w}\right)\cdot\boldsymbol{\mu}^{*}\,d\,\Gamma=0$

Expression of the cohesive force $\forall\,\boldsymbol{w}^{*}\in\boldsymbol{M}_{h},-\int_{\Gamma}\left[\boldsymbol{\mu}-\boldsymbol{t}_{c}(\boldsymbol{\lambda}+r\,\boldsymbol{w})\right]\cdot\boldsymbol{w}^{*}\,d\,\Gamma=0$

Law of interface $\forall\,\boldsymbol{\lambda}^{*}\in\boldsymbol{M}_{h},-\int_{\Gamma}\frac{\left[\boldsymbol{\lambda}-\boldsymbol{t}_{c}(\boldsymbol{\lambda}+r\,\boldsymbol{w})\right]}{r}\cdot\boldsymbol{\lambda}^{*}\,d\,\Gamma=0$

4 Strategy of resolution

4.1 Method of Newton-Raphson

The strategy of resolution is not other than a simple method of Newton. Contrary to the case of contact-friction [R5.03.52] or [R5.03.54], there are neither loops of fixed point, nor fields of signs. The only operation to be realized besides the iterations of Newton is thus the actualization of the internal variable.

For a step of time:

- Iterations of Newton

Calculation of the tangent matrix and the second member

- End of the iterations of Newton

Actualization of the internal variable α

One could legitimately wonder why the internal variable is not brought up to date during iterations of Newton. In fact, as it is about a parameter measuring the irreversibility, and determined by a maximum in the course of time, he should be updated only with each step of converged time. Indeed, in the contrary case, if this parameter exceeds its value of balance at the time of an iteration of Newton, the algorithm of Newton will be then unable to decrease it to find the value of balance.

In the unidimensional case, the method of Newton is an iterative process making it possible to approach the zeros of a continuous and derivable function. One is reduced to the resolution of $F(x)=0$. A succession of points is built x^{k} by doing one develop of Taylor of F in the vicinity of x^{k} , which gives to the first order:

$$F\left(x^{k+1}\right)\approx F\left(x^{k}\right)+F'\left(x^{k}\right)\left(x^{k+1}-x^{k}\right)$$

While noting $\delta x^{k}=x^{k+1}-x^{k}$ the increment between two successive iterations, the equation linearized with the iteration $k+1$ is then the following one:

$$F'\left(x^{k}\right)\delta x^{k}=-F\left(x^{k}\right)$$

In the case of the finite element method, $F'(x^k)$ are connected with the tangent matrix, which can be calculated with each iteration so necessary, δx^k is the vector of the increments of the nodal unknown factors, and $F(x^k)$ is the second member. It is noted that $F'(x^k)$ and $F(x^k)$ only quantities of the iteration utilize k, which is thus known quantities.

4.2 Differentiation of the cohesive law

To give an example of differentiation of the cohesive law coupling the modes, let us consider the regularized cohesive law CZM_EXP_REG. Lhas differential $\boldsymbol{t}_c(\llbracket \boldsymbol{u} \rrbracket)$ will be $\frac{\partial \boldsymbol{t}_c}{\partial \llbracket \boldsymbol{u} \rrbracket} \cdot \llbracket \delta \boldsymbol{u} \rrbracket$ with:

However $\frac{\partial \boldsymbol{t}_c}{\partial \llbracket \boldsymbol{u} \rrbracket} = H(\llbracket u \rrbracket_{\text{èq}} - \alpha) \frac{\partial \boldsymbol{\sigma}_{lin}}{\partial \llbracket \boldsymbol{u} \rrbracket} + (1 - H(\llbracket u \rrbracket_{\text{èq}} - \alpha)) \frac{\partial \boldsymbol{\sigma}_{dis}}{\partial \llbracket \boldsymbol{u} \rrbracket} + \frac{\partial \boldsymbol{\sigma}_{pen}}{\partial \llbracket \boldsymbol{u} \rrbracket}$

We re-use the expressions from these three derivative partial which are given in [R7.02.11], with $\boldsymbol{\delta} = \llbracket \boldsymbol{u} \rrbracket$. In the expression of $\boldsymbol{\sigma}_{dis}$, it is necessary to write $\alpha = \llbracket u \rrbracket_{èq}$, which becomes thus a variable to be taken into account in derivation. In practice, in the code, one distinguishes four cases for clearness from reading:

- $\llbracket u \rrbracket_{èq} \geq \alpha$ et $\llbracket u_n \rrbracket \geq 0$ (dissipative lack of contact). We have then:

$$\frac{\partial \boldsymbol{t}_c}{\partial \llbracket \boldsymbol{u} \rrbracket} = \sigma_c \exp\left(-\frac{\sigma_c}{G_c} \llbracket u \rrbracket_{èq}\right) \left(\frac{\mathbf{Id}}{\llbracket u \rrbracket_{èq}} - \frac{\llbracket \boldsymbol{u} \rrbracket}{\llbracket u \rrbracket_{èq}} \otimes \frac{\llbracket \boldsymbol{u} \rrbracket}{\llbracket u \rrbracket_{èq}} \left(\frac{\sigma_c}{G_c} + \frac{1}{\llbracket u \rrbracket_{èq}} \right) \right)$$

- $\llbracket u \rrbracket_{èq} < \alpha$ et $\llbracket u_n \rrbracket < 0$ (contacting rubber band). With $(\boldsymbol{\tau}_1, \boldsymbol{\tau}_2)$ a base of the tangent plan, we have:

$$\frac{\partial \boldsymbol{t}_c}{\partial \llbracket \boldsymbol{u} \rrbracket} = \frac{\partial \boldsymbol{\sigma}_{lin}(\llbracket \boldsymbol{u}_\tau \rrbracket)}{\partial \llbracket \boldsymbol{u} \rrbracket} + \frac{\partial \boldsymbol{\sigma}_{pen}(\llbracket \boldsymbol{u}_n \rrbracket)}{\partial \llbracket \boldsymbol{u} \rrbracket} = C\, \boldsymbol{n} \otimes \boldsymbol{n} + \frac{\sigma_c}{\alpha} \exp\left(\frac{-\sigma_c}{G_c} \alpha\right) (\boldsymbol{\tau}_1 \otimes \boldsymbol{\tau}_1 + \boldsymbol{\tau}_2 \otimes \boldsymbol{\tau}_2)$$

- $\llbracket u \rrbracket_{èq} \geq \alpha$ et $\llbracket u_n \rrbracket < 0$ (dissipative contacting). By a similar reasoning while replacing $\boldsymbol{\sigma}_{lin}$ by $\boldsymbol{\sigma}_{dis}$, we obtain:

$$\frac{\partial \boldsymbol{t}_c}{\partial \llbracket \boldsymbol{u} \rrbracket} = C\, \boldsymbol{n} \otimes \boldsymbol{n} + \exp\left(\frac{-\sigma_c}{G_c} \llbracket u \rrbracket_{èq}\right) \left[\frac{\sigma_c}{\llbracket u \rrbracket_{èq}} (\boldsymbol{\tau}_1 \otimes \boldsymbol{\tau}_1 + \boldsymbol{\tau}_2 \otimes \boldsymbol{\tau}_2) - \left(\frac{\sigma_c^2}{G_c} + \frac{\sigma_c}{\llbracket u \rrbracket_{èq}} \right) \frac{\llbracket \boldsymbol{u} \rrbracket_\tau \otimes \llbracket \boldsymbol{u} \rrbracket_\tau}{\llbracket u \rrbracket_{èq}^2} \right]$$

- $\llbracket u \rrbracket_{èq} < \alpha$ et $\llbracket u_n \rrbracket \geq 0$ (lack of contact rubber band).

$$\frac{\partial \boldsymbol{t}_c}{\partial \llbracket \boldsymbol{u} \rrbracket} = \frac{\sigma_c}{\alpha} \exp\left(\frac{-\sigma_c}{G_c} \alpha\right) \mathbf{Id}$$

4.3 Linearization of the problem

4.3.1 Integral writing for a formulation with regularized cohesive law

The linear system of the three equations to the iteration of Newton $k+1$ is written in the following way (by weighing down the writing, the references to the iteration of Newton are omitted, because in an obvious way, the unknown factors are noted with one δ in front of, and the fields tests from now on are noted with a star):

To find $(\delta u\ ,\ \delta\lambda_n\ ,\ \delta\lambda_\tau)\in V_0\times H\times H$ such as:
$\forall(u^*\ ,\ \lambda_n^*,\ \lambda_\tau^*)\in V_0\times H\times H$

Equilibrium equation
$$\int_\Omega \sigma(\delta u):\varepsilon(u^*)\,d\Omega$$
$$+\int_{\Gamma_c}\left[\frac{\partial t_{c,n}}{\partial[\![u]\!]_n}[\![\delta u]\!]_n+\frac{\partial t_{c,n}}{\partial[\![u]\!]_\tau}[\![\delta u]\!]_\tau\right][\![u^*]\!]_n d\Gamma_c$$
$$+\int_{\Gamma_c}\left[\frac{\partial t_{c,\tau}}{\partial[\![u]\!]_n}[\![\delta u]\!]_n+\frac{\partial t_{c,\tau}}{\partial[\![u]\!]_\tau}[\![\delta u]\!]_\tau\right][\![u^*]\!]_\tau d\Gamma_c$$
$$=-\int_\Omega \sigma(u):\varepsilon(u^*)\,d\Omega+\int_\Omega f\cdot u^*\,d\Omega+\int_{\Gamma_t} t\cdot u^*\,d\Gamma_t$$
$$-\int_{\Gamma_c}\left(t_{c,n}[\![u^*]\!]_n+t_{c,\tau}[\![u^*]\!]_\tau\right)d\Gamma_c$$

Interface: normal part
$$\int_{\Gamma c}\lambda_n^*\left(\lambda_n+\delta\lambda_n-t_c\cdot n\right)d\Gamma_c=0$$

Interface: tangential part
$$\int_{\Gamma c}\lambda_\tau^*\left(\lambda_\tau+\delta\lambda_\tau-t_{c,\tau}\right)d\Gamma_c=0$$

4.3.2 Integral writing for a formulation with mixed cohesive law for quadratic elements

The linear system of the three equations to the iteration of Newton $k+1$ is written in the following way (by weighing down the writing, the references to the iteration of Newton are omitted, because in an obvious way, the unknown factors are noted with one δ in front of, and the fields tests from now on are noted with a star):
To find $(\delta u\ ,\ \delta\lambda\ )\in V_0\times H$ such as:
$\forall(u^*\ ,\ \lambda^*)\in V_0\times H$

Equilibrium equation
$$\int_\Omega \sigma(\delta u):\epsilon(u^*)\,d\Omega+\int_\Gamma\left(Id-r\frac{\partial\delta}{\partial p}\right)\cdot\delta\lambda\cdot[\![u^*]\!]\,d\Gamma$$
$$+\int_\Gamma r\left(Id-r\frac{\partial\delta}{\partial p}\right)\cdot[\![\delta u]\!]\cdot[\![u^*]\!]\,d\Gamma$$
$$=-\int_\Omega \sigma(u):\epsilon(u^*)\,d\Omega+\int_\Omega f\cdot u^*\,d\Omega+\int_{\Gamma_t} t\cdot u^*\,d\Gamma$$
$$-\int_{\Gamma_c}\left[\lambda+r(\ [\![u]\!]-\delta(p)\ )\right]\cdot[\![u^*]\!]\,d\Gamma$$

Law of interface
$$\int_{\Gamma_c}\left(1-r\frac{\partial\delta}{\partial p}\right)\cdot[\![u]\!]\cdot\lambda^*\,d\Gamma-\int_\Gamma\frac{\partial\delta}{\partial p}\cdot\delta\lambda\cdot\lambda*\,d\Gamma$$
$$=-\int_\Gamma([\![u]\!]-\delta)\cdot\lambda^*\,d\Gamma$$

4.3.3 Integral writing for a formulation with mixed cohesive law for linear elements

The linear system to solve for an iteration of Newton is written:
To find $(\delta u\ ,\ \delta\mu\ ,\ \delta w\ ,\ \delta\lambda\ )\in V_0\times H\times H\times H$ such as:
$\forall(u^*,\mu^*,w^*,\lambda^*)\in V_0\times H\times H\times H$

Equilibrium equation
$$\int_\Omega \sigma(\delta\boldsymbol{u}):\epsilon(\boldsymbol{u}^*)\,d\Omega+\int_\Gamma\delta\boldsymbol{\mu}\cdot[\![\boldsymbol{u}^*]\!]\,d\Gamma$$
$$=-\int_\Omega \sigma(\boldsymbol{u}):\epsilon(\boldsymbol{u}^*)\,d\Omega+\int_{\Gamma_g}\boldsymbol{g}\cdot\boldsymbol{u}^*\,d\Gamma_g-\int_\Gamma\boldsymbol{\mu}\cdot[\![\boldsymbol{u}^*]\!]\,d\Gamma$$

Projection of the jump of displacement
$$\int_\Gamma (\llbracket \delta \boldsymbol{u} \rrbracket - \delta \boldsymbol{w}) \cdot \boldsymbol{\mu}^* \, d\Gamma = -\int_\Gamma (\llbracket \boldsymbol{u} \rrbracket - \boldsymbol{w}) \cdot \boldsymbol{\mu}^* \, d\Gamma$$

Cohesive constraint
$$-\int_\Gamma \left[\delta \boldsymbol{\mu} - \frac{\partial \boldsymbol{t}_c}{\partial (\boldsymbol{\lambda} + r \boldsymbol{w})} \cdot (\delta \boldsymbol{\lambda} + r \delta \boldsymbol{w}) \right] \cdot \boldsymbol{w}^* \, d\Gamma$$
$$= \int_\Gamma \left[\boldsymbol{\mu} - \boldsymbol{t}_c (\boldsymbol{\lambda} + r \boldsymbol{w}) \right] \cdot \boldsymbol{w}^* \, d\Gamma$$

Law of interface
$$-\int_\Gamma \left[\frac{\delta \boldsymbol{\lambda}}{r} - \frac{\partial \boldsymbol{t}_c}{\partial (\boldsymbol{\lambda} + r \boldsymbol{w})} \cdot \left(\frac{\delta \boldsymbol{\lambda}}{r} + \delta \boldsymbol{w} \right) \right] \cdot \boldsymbol{\lambda}^* \, d\Gamma$$
$$= \int_\Gamma \frac{\left[\boldsymbol{\lambda} - \boldsymbol{t}_c (\boldsymbol{\lambda} + r \boldsymbol{w}) \right]}{r} \cdot \boldsymbol{\lambda}^* \, d\Gamma$$

5 Ematric xpression of the problem

5.1 Loi cohesive regularized

5.1.1 Matric writing of the linearized problem

By taking again the notations of [R5.03.54], and by considering the unified writing adopted for the laws of contact friction and cohesive regularized, the system linearized such as it is solved with the iteration $k+1$ of Newton can put itself in form matriciit:

Equilibrium equation
$$\left\{u^*\right\}\left[K_{méca}\right](\delta u) + \left\{u^*\right\}\left[K^u_{coh}\right](\delta u) = \left\{u^*\right\}\left(L^1_{méca}\right) + \left\{u^*\right\}\left(L^1_{coh}\right)$$

Postprocessing forced cohesive normal
$$\left\{\lambda^*_n\right\}[C](\delta\lambda_n) = \left\{\lambda^*_n\right\}\left(L^1_{post}\right) + \left\{\lambda^*_n\right\}\left(L^2_{coh}\right)$$

Postprocessing forced cohesive tangential
$$\left\{\lambda^*_\tau\right\}\left[F_r\right](\delta\lambda_\tau) = \left\{\lambda^*_\tau\right\}\left(L^2_{post}\right) + \left\{\lambda^*_\tau\right\}\left(L^3_{coh}\right)$$

where the vectors column are noted (x) and the vectors line $\{x\} = (x)^T$. This system can be put in the following matric form:

$$\begin{bmatrix} K_{méca} + K^u_{coh} & 0 & 0 \\ 0 & C & 0 \\ 0 & 0 & F \end{bmatrix} \begin{pmatrix} \delta u \\ \delta\lambda_n \\ \delta\lambda_\tau \end{pmatrix} = \begin{pmatrix} L^1_{méca} + L^1_{coh} \\ L^1_{post} + L^2_{coh} \\ L^2_{post} + L^3_{coh} \end{pmatrix}$$

The unknown factor is the increment compared to the preceding iteration of Newton. One voluntarily omitted reference to the number of the iteration of Newton.

$K_{méca}$ is the mechanical matrix of rigidity defined in the paragraph [§3.2] of [R7.02.12].
K^u_{coh} is the matrix of rigidity due to the forces of cohesion.
C is the matrix of postprocessing for the normal direction.
F is the matrix of postprocessing for (them) the direction (S) tangential (S).
$L^1_{méca}$ is the second member representing the internal forces and the increments of loadings.
L^1_{post} and L^2_{post} are the second members of postprocessing.
L^1_{coh} , L^2_{coh} and L^3_{coh} are the second members due to the forces of cohesion.

Note:

It is pointed out that the system solved by Code_Aster is not of the type $[K][U]=[F]$ but of the type $[K][U]+[F]=0$. There thus exists a minus sign between the second members given in this document and those coded in files FORTRAN.

5.1.2 Expression of the matrices and elementary vectors

The matrix C necessary to postprocessing has as an expression (the indices n on λ, to indicate the normal component of the cohesive constraint, are omitted):

$$\left\{\lambda^*\right\}_i\left[C\right]_{ij}\left(\delta\lambda\right)_j=\int_\Gamma \psi_i\,\lambda_i^*\,\psi_j\,\delta\lambda_j\,d\Gamma$$

The vector L^1_{post} necessary to postprocessing has as an expression (indices n omitted on on λ):

$$\left\{\lambda^*\right\}_i\left(L^1_{post}\right)_i=\int_\Gamma \psi_i\,\lambda_i^*\,\lambda^{k-1}\,d\Gamma$$

matrix F necessary to postprocessing has as an expression:

$$\left\{\lambda_\tau^*\right\}_i\left[F\right]_{ij}\left(\delta\lambda_\tau\right)_j=\int_\Gamma \psi_i\left\{\lambda^{1*}_{\tau,i}\quad\lambda^{2*}_{\tau,i}\right\}\cdot\begin{bmatrix}\tau_i^1\tau_j^1 & \tau_i^1\tau_j^2\\ \tau_i^2\tau_j^1 & \tau_i^2\tau_j^2\end{bmatrix}\cdot\psi_j\begin{Bmatrix}\lambda^1_{\tau,j}\\ \lambda^2_{\tau,j}\end{Bmatrix}d\Gamma$$

The vector L^2_{post} necessary to postprocessing has as an expression:

$$\left\{\lambda_\tau^*\right\}_i\left(L^2_{post}\right)_i=\int_\Gamma \psi_i\left\{\lambda^{1*}_{\tau,i}\tau_i^1+\lambda^{2*}_{\tau,i}\tau_i^2\right\}\lambda_\tau^{k-1}\,d\Gamma$$

Now let us seek to write K^u_{coh}. Are two directions of the fixed base X and Y, unit vectors $\boldsymbol{e}_X$ and $\boldsymbol{e}_Y$. Let us introduce the tangent matrix of the cohesive law into the fixed base $\boldsymbol{K}^{gl}$ coefficients $K^{gl}_{XY}=\boldsymbol{e}_X\cdot\dfrac{\partial\boldsymbol{t}_c}{\partial[\![\boldsymbol{u}]\!]}\cdot\boldsymbol{e}_Y$. With the expression of $\dfrac{\partial\boldsymbol{t}_c}{\partial[\![\boldsymbol{u}]\!]}$ data with [the §4.2], we have the tangent matrix of the cohesive law $\boldsymbol{K}^{loc}$ in the local base (see Doc. [R7.02.11]). We obtain then $\boldsymbol{K}^{gl}$ by $\boldsymbol{K}^{gl}=\boldsymbol{Q}^T\cdot\boldsymbol{K}_{loc}\cdot\boldsymbol{Q}$, where $\boldsymbol{Q}$ is an orthonormal matrix of passage defined by:

$$\boldsymbol{Q}=\begin{bmatrix}n_X & n_Y & n_Z\\ \tau^1_X & \tau^1_Y & \tau^1_Z\\ \tau^2_X & \tau^2_Y & \tau^2_Z\end{bmatrix}$$

Are i and j two nodes nouveau riches. That is to say Γ the intersection of the supports of i and j. The matrix $[K^u_{coh}]$ is then given by:

$$\{u^*\}_i[K^u_{coh}]_{ij}\{\delta u\}_j=\int_\Gamma 2\,\varphi_i\,\boldsymbol{b}_i^*\cdot\boldsymbol{K}^{gl}\cdot\boldsymbol{b}_j\,2\,\varphi_j\,d\,\Gamma$$

The second members of cohesion have the following expressions:

$$\{u_i\}^*\left(L^1_{coh}\right)_i=-\int_\Gamma 2\,\varphi_i\,\boldsymbol{b}_i^*\cdot\boldsymbol{t}_c^{k-1}\,d\,\Gamma$$

where one can express $\boldsymbol{t}_c$ in the total base by $\boldsymbol{t}_c^{glo}=\boldsymbol{Q}^T\cdot\boldsymbol{t}_c^{loc}$, and:

$$\left\{\lambda_n^*\right\}_i\left(L^2_{coh}\right)_i=-\int_\Gamma \psi_i\,\lambda^*_{n,i}\left(t^{k-1}_{c,n}\right)d\Gamma$$

$$\left\{\lambda_\tau^*\right\}_i\left(L^3_{coh}\right)_i=-\int_\Gamma \psi_i\left\{\lambda^{1*}_{\tau,i}\boldsymbol{\tau}_i^1+\lambda^{2*}_{\tau,i}\boldsymbol{\tau}_i^2\right\}\cdot\boldsymbol{t}^{k-1}_{c,\tau}\,d\Gamma$$

where $k-1$ represent the index of the preceding iteration of Newton.

5.2 Mixed cohesive law for quadratic elements

5.2.1 Ematric criture of the problem with mixed cohesive law

The matric system such as it is solved with the iteration $k+1$ of Newton can put itself in following matric form:

$$\begin{bmatrix} K_{méca}+A_u & A^T \\ A & C \end{bmatrix} \begin{pmatrix} \delta u \\ \delta\lambda \end{pmatrix} = \begin{pmatrix} L^1_{méca}+L^1_{coh} \\ L^2_{coh} \end{pmatrix}$$

5.2.1.1 Form of the elementary matrices of cohesion:

Are two directions of the fixed base X and Y, unit vectors $\boldsymbol{e}_X$ and $\boldsymbol{e}_Y$. We introduce as previously the tangent matrix of the cohesive law into the fixed base $\boldsymbol{K}^{gl}$ coefficients $K^{gl}_{XY}=\boldsymbol{e}_X\cdot\frac{\partial\boldsymbol{\delta}}{\partial\boldsymbol{p}}\cdot\boldsymbol{e}_Y$. We lay out, by the cohesive law of behavior, of the tangent matrix $\boldsymbol{K}_{loc}$ in the local base (see Doc. [R7.02.11]). We obtain then $\boldsymbol{K}_{gl}$ by $\boldsymbol{K}^{gl}=\boldsymbol{Q}^T\cdot\boldsymbol{K}^{loc}\cdot\boldsymbol{Q}$, where $\boldsymbol{Q}$ is an orthonormal matrix of passage defined by:

$$\boldsymbol{Q}=\begin{bmatrix} n_X & n_Y & n_Z \\ \tau^1_X & \tau^1_Y & \tau^1_Z \\ \tau^2_X & \tau^2_Y & \tau^2_Z \end{bmatrix}$$

Having introduced these notations, we have:

$$\{u^*\}_i[A_u]_{ij}\{\delta u\}_j=\int_\Gamma 2\varphi_i b_i^* r\left(\mathbf{1}-r\,\boldsymbol{K}^{gl}\right)2\varphi_j b_j d\Gamma$$

In addition, we choose to discretize $\boldsymbol{\lambda}$ in local base. The coefficient $(1,1)$ matrix $\{\lambda_n^*\}[A_u]_{ij}\{\delta u_X\}_j$ is then $\int_\Gamma \varphi_i\lambda_i^*\boldsymbol{n}\cdot\left(\mathbf{1}-r\frac{\partial\boldsymbol{\delta}}{\partial\boldsymbol{p}}\right)\cdot\boldsymbol{e}_X 2\varphi_j b_j d\Gamma$. For the coefficients $(2,1)$ and $(3,1)$, the formula is the same one while replacing $\boldsymbol{n}$ by $\boldsymbol{\tau}_1$ and $\boldsymbol{\tau}_2$, respectively. By exploiting the notations introduced into the preceding paragraph, we deduce some:

$$\{\lambda^*\}_i[A]_{ij}\{\delta u\}_j=\int_\Gamma \varphi_i\lambda_i^*\left(\mathbf{1}-r\,\boldsymbol{K}^{loc}\right)\cdot\boldsymbol{Q}\,2\varphi_j b_j d\Gamma$$

As for the matrix $[C]$, she is written simply:

$$\{\lambda^*\}_i[C]_{ij}\{\delta\lambda\}_j=-\int_\Gamma \varphi_i\lambda_i^*\boldsymbol{K}^{loc}\varphi_j\lambda_j d\Gamma$$

5.2.1.2 Expression of the elementary vectors of cohesion:

The coefficient according to X of $\left(L^1_{coh}\right)_i$ has as an expression $\int_\Gamma\varphi_i\left(-\boldsymbol{\lambda}\cdot\boldsymbol{e}_X-r\left(\llbracket\boldsymbol{u}\rrbracket-\boldsymbol{\delta}\right)\cdot\boldsymbol{e}_X\right)d\Gamma$. With the notations indroduites in the preceding ones part, we deduce:

$$\{u_i\}^*\left(L^1_{coh}\right)_i=\int_\Gamma 2\varphi_i\boldsymbol{b}_i^*\cdot\left(-\boldsymbol{Q}^T\cdot\boldsymbol{\lambda}-r\ \left(\llbracket\boldsymbol{u}\rrbracket-\boldsymbol{Q}^T\cdot\boldsymbol{\delta}\right)\ \right)d\Gamma$$

where $\boldsymbol{\delta}$ and $\boldsymbol{\lambda}$ are given in local base, and $\llbracket\boldsymbol{u}\rrbracket$ in fixed base.

The coefficient 1 of $\left(L^2_{coh}\right)_i$ is written $\int_\Gamma\left(-\llbracket\boldsymbol{u}\rrbracket\cdot\boldsymbol{n}+\boldsymbol{\delta}\cdot\boldsymbol{n}\right)d\Gamma$. For the coefficients 2 and 3, the formula is the same one while replacing $\boldsymbol{n}$ by $\boldsymbol{\tau}_1$ and $\boldsymbol{\tau}_2$, respectively. We deduce some:

$$\{\lambda\}_i^*\left(L_{coh}^2\right)_i=\int_\Gamma \boldsymbol{\lambda}_i^*\cdot\left(-\boldsymbol{Q}[\![\boldsymbol{u}]\!]+\boldsymbol{\delta}\right)d\Gamma$$

where $\boldsymbol{\delta}$ is given in local base, and $[\![\boldsymbol{u}]\!]$ in fixed base.

5.3 Mixed cohesive law for linear elements

Components of the unknown factors $\boldsymbol{u}$ and $\boldsymbol{\mu}$ are defined in a fixed base $\left(\boldsymbol{e}_X,\boldsymbol{e}_Y,\boldsymbol{e}_Z\right)$, while components of $\boldsymbol{w}$ and $\boldsymbol{\lambda}$ are defined in the local base $\left(\boldsymbol{n},\boldsymbol{\tau}_1,\boldsymbol{\tau}_2\right)$ on fissured surface Γ in each point $\boldsymbol{x}\in\Gamma$, so that :

$$\boldsymbol{w}(\boldsymbol{x})=\sum_{i=1}^{N_\lambda}\psi_I(\boldsymbol{x})\left(w_{I,n}\boldsymbol{n}(\boldsymbol{x})+w_{I,\tau 1}\boldsymbol{\tau}_1(\boldsymbol{x})+w_{I,\tau 2}\boldsymbol{\tau}_2(\boldsymbol{x})\right)$$

A similar definition is worth for $\boldsymbol{\lambda}$. For a degree of freedom I reduced space (see §3.3), it is possible to determine the components $t_{c,n}^I,t_{t,\tau 1}^I,t_{c,\tau 2}^I$ cohesive force from $\left(w_{I,n},w_{I,\tau 1},w_{I,\tau 2}\right)$, $\left(\lambda_{I,n},\lambda_{I,\tau 1},\lambda_{I,\tau 2}\right)$ and of the cohesive law of the §2.2.3. These components are not intended to be associated with a particular direction I degree of freedom, but intended to be connected to the weak direction for the total constraint $\boldsymbol{\mu}$ written in fixed base.
The matric system can be put in the following form:

$$\begin{bmatrix} K^{uu} & \left(K^{\mu u}\right)^T & 0 & 0 \\ K^{\mu u} & 0 & \left(-K^{w\mu}\right)^T & 0 \\ 0 & -K^{w\mu} & D^{ww} & \left(D^{\lambda w}\right)^T \\ 0 & 0 & D^{\lambda w} & D^{\lambda\lambda} \end{bmatrix}\begin{pmatrix}\delta u\\ \delta\mu\\ \delta w\\ \delta\lambda\end{pmatrix}=\begin{pmatrix} L_{\text{méca}}+L_\mu^1\\ L_u-L_w\\ -L_\mu^2+L_{coh}^1\\ -L_\lambda+L_{coh}^2\end{pmatrix}$$

where:

– K^{uu} is the voluminal matrix of rigidity;

– $K^{\mu u}$ and $K^{w\mu}$ are matrices discretizing the operators “mortar”, the last one also managing the basic change;

– matrices D are all diagonal per blocks: for I and J two distinct DDL of Lagrange, they check $D_{IJ}=0$.

Let us give the expressions of the matrices and second members who do not depend on the cohesive law:

$$\{u\}_i^*\left[K^{\mu u}\right]_{iJ}\left(\delta\mu\right)_J=\boldsymbol{b}_i^*\cdot\left(\delta\boldsymbol{\mu}_J\right)\int_\Gamma 2\,\psi_J\varphi_i\,d\Gamma$$

By introducing the matrix of basic change orthonormal $\boldsymbol{Q}$ defined as previously, we have:

$$\{w\}_I^*\left[K^{w\mu}\right]_{IJ}\left(\delta\mu\right)_J=\boldsymbol{w}_I^*\cdot\left(\int_\Gamma\psi_I\psi_J\boldsymbol{Q}\,d\Gamma\right)\cdot\left(\delta\boldsymbol{\mu}_J\right)$$
$$\{u\}_i^*\left(L_\mu^1\right)_i=-\boldsymbol{b}_i^*\cdot\int_\Gamma 2\varphi_i\boldsymbol{\mu}\,d\Gamma$$
$$\{\mu\}_I^*\left(L_u\right)_I=-\boldsymbol{\mu}_I^*\cdot\int_\Gamma\psi_I[\![\boldsymbol{u}]\!]d\Gamma$$
$$\{\mu\}_I^*\left(L_w\right)_I=-\boldsymbol{\mu}_I^*\cdot\int_\Gamma\psi_I\boldsymbol{Q}^T\cdot\boldsymbol{w}\,d\Gamma$$
$$\{w\}_I^*\left(L_\mu^2\right)_I=\boldsymbol{w}_I^*\cdot\int_\Gamma\psi_I\boldsymbol{Q}\cdot\boldsymbol{\mu}\,d\Gamma$$

Let us detail now the discretization of the quantities of interface. The matrices are diagonal per blocks, and have as expressions:

$$\{w\}_I^*\left[D^{ww}\right]_{II}(\delta w)_I=w_I^*(\delta w_I)r\frac{\partial \boldsymbol{t}_c}{\partial(\boldsymbol{\lambda}+r\boldsymbol{w})}(\lambda_I+r w_I)\int_\Gamma \psi_I d\Gamma$$

$$\{\lambda\}_I^*\left[D^{\lambda w}\right]_{II}(\delta w)_I=\lambda_I^*(\delta w_I)\frac{\partial \boldsymbol{t}_c}{\partial(\boldsymbol{\lambda}+r\boldsymbol{w})}(\lambda_I+r w_I)\int_\Gamma \psi_I d\Gamma$$

$$\{\lambda\}_I^*\left[D^{\lambda\lambda}\right]_{II}(\delta\lambda)_I=\lambda_I^*(\delta\lambda_I)\frac{1}{r}\left(\frac{\partial \boldsymbol{t}_c}{\partial(\boldsymbol{\lambda}+r\boldsymbol{w})}(\lambda_I+r w_I)-\mathbf{1}\right)\int_\Gamma \psi_I d\Gamma$$

The elementary vectors have as expressions:

$$\{w\}_I^*\left(L_{coh}^1\right)_I=w_I^*\boldsymbol{t}_c(\lambda_I+r w_I)\int_\Gamma \psi_I d\Gamma$$

$$\{w\}_I^*\left(L_{coh}^2\right)_I=\frac{w_I^*}{r}\boldsymbol{t}_c(\lambda_I+r w_I)\int_\Gamma \psi_I d\Gamma$$

6 Propagation of a cohesive crack

In this method, models of cohesive zones are introduced on potential surfaces of cracking wide. Thus, the cohesive law will naturally separate the fields adherent and open, which requires a formulation for the cohesive law which allows a faithful representation of adherent zones of big size. The problem was discussed with the §3. An implicit actualization of the face of propagation can then be carried out, which makes the originality of the method suggested here. For the algorithms of propagation, we use a mixed cohesive law with linear elements CZM_LIN_MIX, which is introduced into the model by the order DEFI_CONTACT, with the keyword ZONE/RELATION.

Let us suppose a structure having a fissured surface, described by a cohesive law, for which one knows the cohesive face separating the effective zone cohesive from the potential surface of cracking, i.e. surface within which the crack will be able to be propagated with the next step of loading (see fig.6-a). The realization of an iteration of the calculation of propagation then comprises, in the order, the following stages (see fig.6-a):

a) the realization of mechanical calculation to the step of next time (order STAT_NON_LINE),

b) the detection of the new cohesive face (order PROPA_FISS, operation DETECT_COHESIF),

c) determination of the direction of propagation along this new face (order CALC_G),

d) the construction of a new zone of potential cracking beyond this face, starting from the directions determined into c), according to an extension length fixes (order PROPA_FISS, operation PROPA_COHESIF),

e) the actualization of the model following this new zone (order MODI_MODELE_XFEM), and if necessary, the projection of the cohesive state running on this new model (keyword ETAT_INIT/COHE in STAT_NON_LINE). This state will be used as initial state for the mechanical calculation of the stage a) of the following iteration.

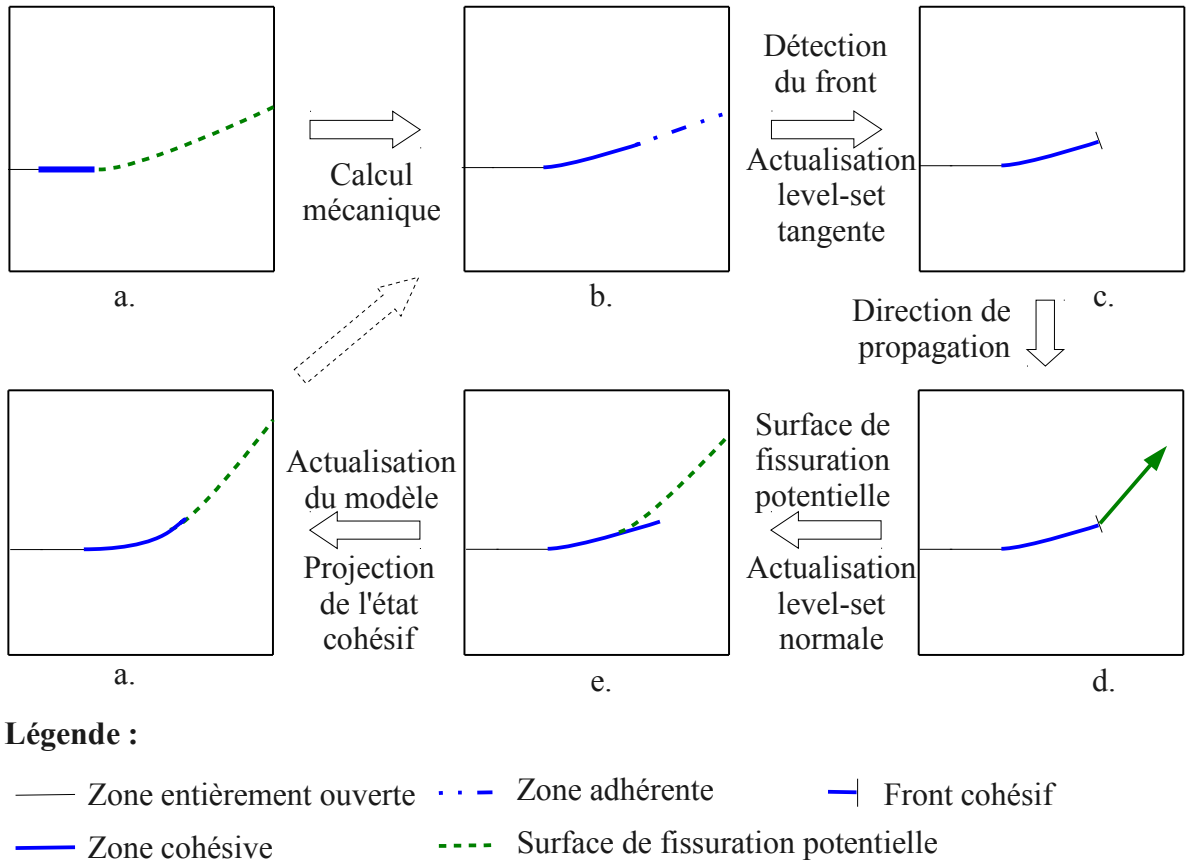

Figure 6-a : Propagation of a crack on unknown way: stages for the realization of a step of propagation.

6.1 Description of a cohesive crack

In order to be able to locate the cohesive face, one defines a discontinuity of the type 'COHESIVE'in DEFI_FISS_XFEM. Compared to a discontinuity of the type 'INTERFACE', it must contain extra information for *to locate the cohesive face:* structures of relative data to the description of a face (coordinated points, bases covariante…) and an additional level-set. Indeed, knowing that the position of the surface of potential cracking is described with a level-set normal by $[\varphi_n = 0]$, the cohesive face is classically located by a level-set additional "tangent", like $[\varphi_n = 0] \cap [\varphi_t = 0]$ (see fig.6.1-a). For a detailed description of the use of level-sets with XFEM, to see documentation [R7.02.12], §2.

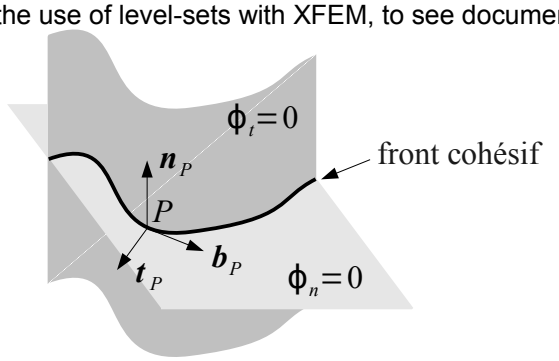

Figure 6.1-a : Description of the cohesive face via level-sets.

Contrary to the type 'CRACK', the type'COHESIVE'does not have singular enrichment in point, because of regularity of the cohesive fields. The zone of potential cracking thus stops on the faces (in 3D) or the edges (in 2D, to see fig.6.1-b) elements.

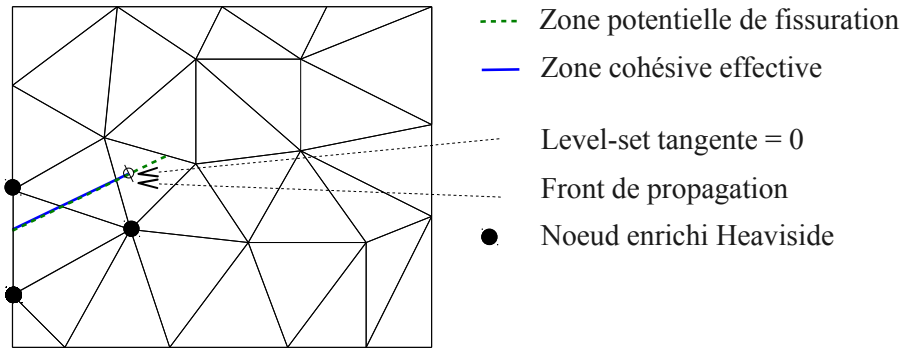

Figure 6.1-b : Characteristics of a crack of the type COHESIVE , at exit of an operation DETECT_COHESIF of PROPA_FISS

Note:

In fact, for the type COHESIVE, the face of propagation necessarily always does not coincide with the Iso-zero of level-set tangent. Indeed, at the time as of phases of mechanical calculation (stage has fig.6-a), the Iso-zero of level-set tangent is used to locate the end of the potential zone of cracking, and thus of enrichment (see fig.6.1-c), while the face of propagation always locates the cohesive face (from which the interface is actually opened, to see fig.6.1-c).

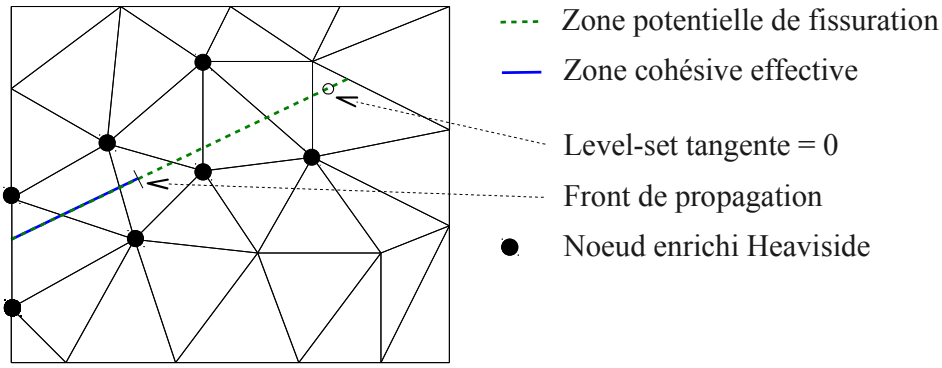

Figure 6.1-c : Characteristics of a crack of the type COHESIVE , at exit of an operation PROPA_COHESIF of PROPA_FISS

Notice – initialization of the procedure:

The initialization of a study of propagation (by the stage has fig. 6-a) is done by giving a potential zone of cracking and an initial face of propagation (see fig. 6.1-d). This last can correspond to a corner of the structure, a simple line on a free edge, or a bottom of preexistent crack (in this last case, this one must be with a grid). In practice, one defines an initial discontinuity of type COHESIVE by DEFI_FISS_XFEM (see fig. 6.1-d) . The initial face is indicated by the keyword GROUP_MA_BORD .

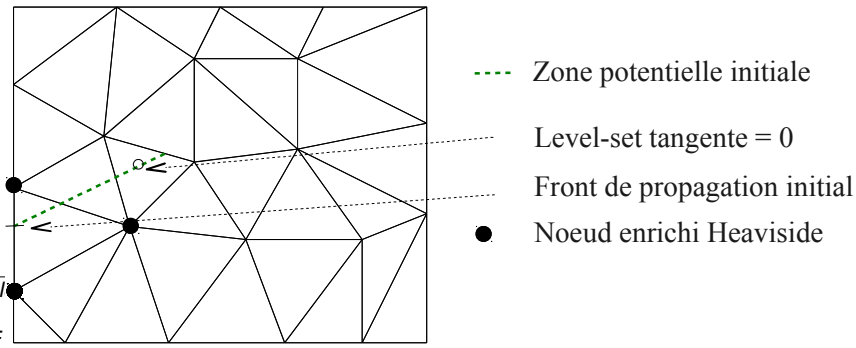

Figure 6.1-d : Characteristics of a crack of the type COHESIVE , at exit of an order DEFI_FISS_XFEM

6.2 Realization of mechanical calculation

The law CZM_LIN_MIX and the formulation used were detailed in the first five parts of this documentation. The length of the cohesive zone is estimated by $l_c=\frac{E G_c}{(1-\nu^2)\sigma_c^2}$. It is advised to choose a size of mesh h such as $l_c \sim \text{quelques}\, h$ so that the cohesive zone is well solved.

It is advised to use the piloting of the loading, which makes it possible to control the projection of crack to each step of propagation. Indeed, in a general way, when the piloting of the loading is used, the increment of displacement Δu is related to the step of time Δt by the relation (see documentation [R5.03.80]):

$$f(\Delta u)=\frac{\Delta t}{\text{COEF\_MULT}}$$

where:
– f is the function of piloting, which depends on the quantity on one seeks to control,
– COEF_MULT is the value indicated under the keyword of the same name, the keyword factor PILOTING order STAT_NON_LINE.

More particularly for the cohesive law CZM_LIN_MIX, the function of piloting is:

$f(\Delta u)=\frac{[\![\Delta u]\!]}{w_c}$ where $w_c=\frac{2G_c}{\sigma_c}$ is the critical jump of displacement.

The length of crack created on a step of propagation is thus roughly $\Delta l=\frac{l_c}{2}\frac{\Delta t}{\text{COEF\_MULT}}$. Once more, it is advised to choose $\Delta l \sim \text{quelques}\, h$. If possible, Δl must be much lower than the radius of curvature expected for fissured surface (in order to collect the geometry of the crack precisely). Failing this, this criterion must be checked a posteriori.

6.3 Detection of the face

In order to determine the face of crack starting from the cohesive computation result, we will allot to the nodes of the grid a statute to know if they healthy or are already damaged. This statute must be a scalar and not be modified in situations of discharge. Consequently, it seems natural to use the internal variable α cohesive law. However, like any internal variable measuring an irreversible process, α do not evolve during the adherent phases ($\alpha=0$, to see §2.2.3). In the state, it thus does not make it possible to determine a scalar field whose Iso-zero would define the face of crack. On the other hand, one can use for this purpose the quantity $\tilde{\alpha}$, such as $\alpha=P_{[0,1]}(\tilde{\alpha})$. For recall (cf §2.2.3), one has $\tilde{\alpha}(t)=\max_{[0,t]}\phi\left((\lambda+r w)_{eq}\right)$ with $\phi\left((\lambda+r w)_{eq}\right):=\frac{(\lambda+r w)_{eq}-\sigma_c}{r w_c-\sigma_c}$. Consequently, $\tilde{\alpha}\leq 0$ corresponds to a healthy material, and $\tilde{\alpha}\geq 0$ with a fissured material.

The construction of a face of crack starting from the preceding relevant field is done while assimilating $\tilde{\alpha}$ with a level-set tangent ϕ_t. The procedure consists then with:

1. to recover the field $\tilde{\alpha}$, already definite like a field with the nodes for the mixed formulation with linear elements;

2. to locate the elements intersected (see fig.6.3-a, stages has and b) by the Iso-zero of $\tilde{\alpha}$. For the detail, to see documentation [R7.02.12], § 3.2.5.1 and § 3.2.5.2;
3. to determine the points of intersection of the Iso-zero of the field with the faces (see fig.6.3-ac). For a detail of the procedure, to see documentation Code_Aster [R7.02.12], §2.4.1.

As highlighted with the references to Code_Aster documentation, all the routines carrying out these operations already exist, considering the field acts like a level-set tangent, which the implementation makes particularly fast.

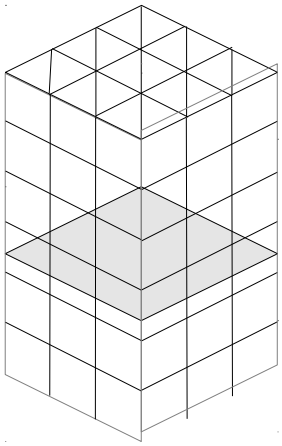

Sights: representations in plan of cut of fissured surface intersecting the grid

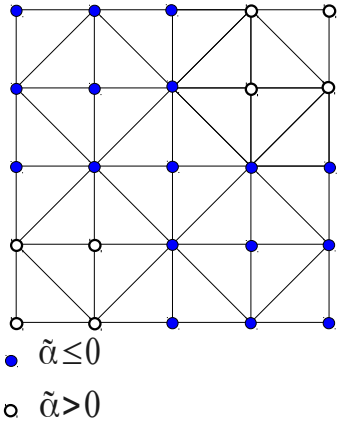

a. nodal values of the internal variable, but negative values if healthy material

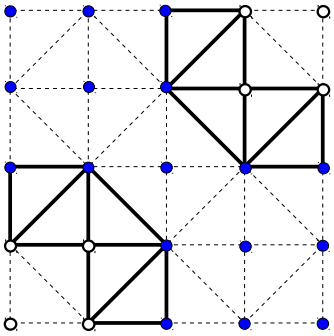

b. determination of the elements intersected by the Iso-zero

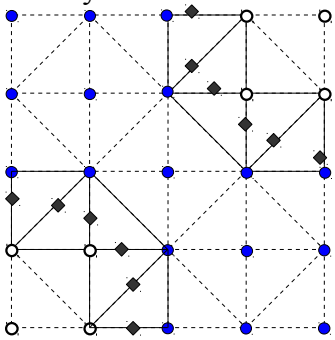

c.points of intersection with the faces of the grid

Figure 6.3-a: Calculation of the levels sets to the nodes projected on the bottom of crack.

Pre-necessary for the phase of detection is the production of a level-set tangent ϕ_t regular: it must be able the being sufficiently to be used by the algorithms of propagation of crack to the following steps of propagation. The field $\varphi_t = \tilde{\alpha}$ and the face which results from this are still too irregular for this use.

In order to gum these irregularities, it is advisable to apply to the face a procedure of smoothing.

With this intention, we use the knowledge of the old face, supposed more regular. The projection of crack which produces the face lately detected from the old one is a posteriori given (fig.a-b). The direction being known starting from the preceding propagation, one applies an algorithm of actualization of level-sets to produce a level-set more regular tangent (fig.Cd).

In detail, the stages of this procedure are given below.

1. For each point P *old* face, one determines a distance from propagation by calculating the distance separating P point of intersection enters the plan $\left(P,\boldsymbol{n}_P,\boldsymbol{t}_P\right)$ and the face “gross” lately detected (see fig.6.3-b, stage a). Being given a length of influence d , Cette distance is calculated in the following way:

$$A_P=\frac{\sum_i \omega(d_i)\,A_i}{\sum_i \omega(d_i)} \text{ with } \omega(d_i)=\left\{\begin{array}{l}\exp\left(\frac{-d_i^2}{2\,d^2}\right) \text{ si } d_i\leq 2\mathrm{d}\\ 0 \text{ sinon}\end{array}\right.$$

Warning. Attention, this is to be distinguished from a projection 3D from P on the new face, which would not provide the same result. In our case, one seeks well the projection in the normal plan with the old face passing by P .

2. One smoothes the field of the standards speed thus obtained (see fig.6.3-b, stage b).

Remarks. If the field is sufficiently regular, this stage could be omitted. Direction of propagation having been given to the step of previous time (see part 6.4), one completely knows the propagation velocity on the old face (see fig.6.3-b, stage c), which allows:

3. The implementation of an algorithm of actualization of the level-sets (see part 6.5), for which one carries out only the operations concerning the level-set tangent (see fig.6.3-b, stage d).

Conclusion. The level-set brought up to date tangent provides the position of a regular face and the associated base covariante.

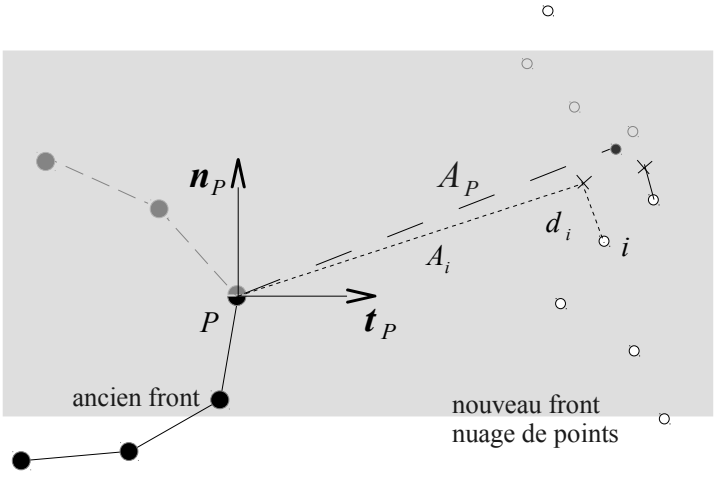

a. reconstruction d'une avancée de fissure le long de l'ancien front

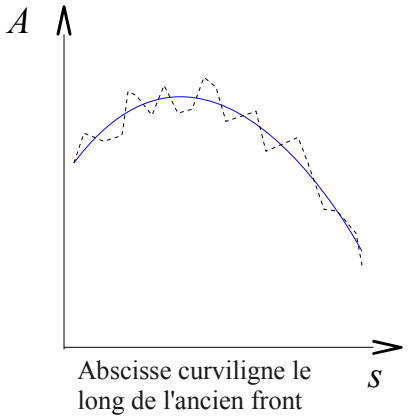

b. lissage de cette avancée

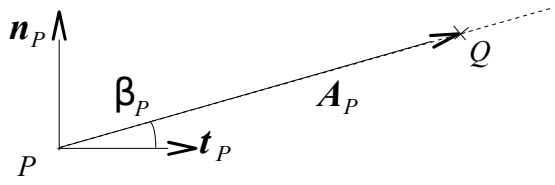

c. déduction de l'avancée vectorielle, l'angle de bifurcation β_P étant disponible depuis l'étape de propagation précédente

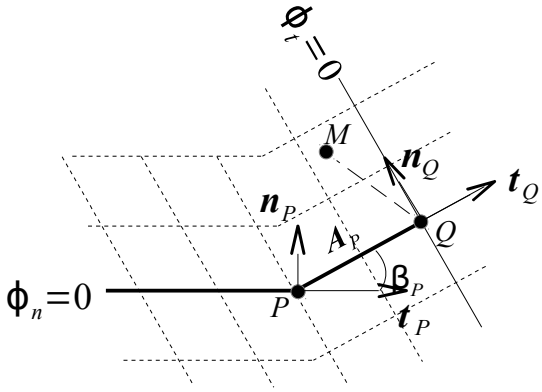

d.mise à jour de la level-set tangente avec l'agorithme de propagation GEOMETRIQUE

Figure 6.3-b: Smoothing of the face of crack.

-

Notice – in connection with the projection of crack at the points ends:

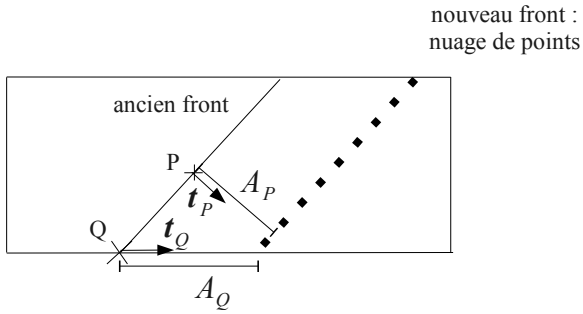

vue de dessus de la surface fissurée

Figure 6.3-c: Advanced of crack at the points ends.

At the time of the determination of the projection of crack a posteriori, one does not take account of the values for the points ends of the old face. Indeed, the base covariante (n_P, t_P) there is corrected to be tangent at free surface (see §6.5). Following this operation, the value of the projection can be there appreciably different from the values at the close points (see fig.6.3-c), which

causes to distort the algorithm of propagation which follows (fig. 6.3-b, stage d). Instead of calculating advanced for these points, one allots the value of the point to them of which propagated remains inside nearest.

Notice – choice length of influence d :

In order to limit the deparameters number having to be regulated by the user, d is automatically deduced from the parameter NB_POINT_FOND given in argument to the procedure PROPA_FISS and with the order CALC_G, by $d=\frac{|T|}{\text{NB\_POINT\_FOND}}$ where $|T|$ is the length of the face of crack.
One can use a parameter NB_POINT_FOND different from step from propagation with another (for example if the face increases), but this adjustment remains at the discretion of the user, it is not automatic. Once more, it is advised to choose $d\sim \text{quelques}\, h$. If possible, d must be much lower than the radii of curvatures expected at the same time for fissured surface and the face (in order to collect their respective geometries precisely). Failing this, this criterion must be checked a posteriori.

6.4 Determination of the direction of propagation

In the literature, the direction of propagation can be deduced from two types of information: either stress fields in the vicinity of the point, or factors of intensity of the constraints equivalents.

The re-use of directional criteria based on the factors of intensity of the constraints even for cohesive calculations was suggested by [bib4, bib5]. The authors explain there that it is about a reasonable assumption for the concrete, since the experiments show that the way of cracking, contrary to the response curve forces/displacement, is almost not sensitive in keeping with the cohesive zone. One could calculate these factors of intensity of the constraints starting from an elastic design of additional free crack – one removes the cohesive forces of the model – as in [bib6, bib7].

One can however do without this additional stage: for example, Moës and Belytschko [bib8] calculate them directly starting from the result with cohesive forces. The argument justifying this simplification is the following (Planed and Elices [bib9]): far from the cohesive zone, the mechanical fields are close to those those of a free crack “equivalent”. Factors of intensity of the constraints *équivalents* can then be defined by integrals of contour which surround totality of the cohesive zone.

We define a virtual field of extension of the crack $\boldsymbol{\theta}$, such as $\|\theta\|=1$, tangent on the surface fissured in each point of this one and directed according to $\boldsymbol{t}$ along the face (see figures 6.4-a and 6.4-c). That is to say C a contour which surrounds totality of the cohesive zone, and Γ_C the part of Γ who is located between the face of crack and the ends of C (see fig.6.4-a), so that $C\cup\Gamma_C^+\cup\Gamma_C^-$ is one contour closed (fig.6.4-a). Like detailed in [bib8], an integral J can be defined on this contour closed like $J=J_{\text{coh}}+J_{\text{ext}}$ with $J_{\text{ext}}:=-\int_C \boldsymbol{\theta}\cdot\boldsymbol{E}\cdot\boldsymbol{n}\,d\Gamma$ and $J_{\text{coh}}=\int_{\Gamma_c}\boldsymbol{\theta}\cdot[\![\boldsymbol{E}]\!]\cdot\boldsymbol{n}\,d\Gamma$, the tensor of Eshelby being noted $\boldsymbol{E}=\nabla\boldsymbol{u}^T\cdot\boldsymbol{\sigma}-\frac{1}{2}\left(\boldsymbol{\sigma}:\boldsymbol{\epsilon}\right)\mathbf{1}$ and $[\![\boldsymbol{E}]\!]=\boldsymbol{E}^+-\boldsymbol{E}^-$. Owing to the fact that $\boldsymbol{\sigma}^+\cdot\boldsymbol{n}=\boldsymbol{\sigma}^-\cdot\boldsymbol{n}=\boldsymbol{t}_c$ and $\boldsymbol{\theta}\cdot\boldsymbol{n}=0$ (for recall, $\boldsymbol{n}$ is directed of $^-$ towards $^+$), the expression of J_{coh} is reduced to:

$$J_{\text{coh}}=\int_{\Gamma_c}\boldsymbol{t}_c\cdot\nabla[\![\boldsymbol{u}]\!]\cdot\boldsymbol{\theta}\,d\Gamma$$

The intégrande of J_{coh} cancel yourself apart from the cohesive zone, since $\boldsymbol{t}_c=0$ on *open zone* and $[\![\boldsymbol{u}]\!]=0$ on *adherent zone*. Thus, J_{coh} is independent of contour C provided that this last surrounds the cohesive zone, and is written like:

$$J_{\text{coh}}=\int_{\Gamma}\boldsymbol{t}_c\cdot\nabla[\![\boldsymbol{u}]\!]\cdot\boldsymbol{\theta}\,d\Gamma$$

Moreover, since there is no singularity in the vicinity of the face in the presence of cohesive forces, we have $J=0$, which confirms that J_{ext} does not depend on C as long as this last includes the cohesive zone.

By the formula of Irwin, we have in addition $J_{\text{ext}}=-J_{\text{coh}}=\frac{1-\nu^2}{E}\left(K_{I,eq}^2+K_{II,eq}^2\right)+\frac{1}{2\mu}K_{III,eq}^2$.

By breaking up the cohesive force by $\boldsymbol{t}_c=t_{c,n}\boldsymbol{n}+t_{c,t}\boldsymbol{t}+t_{c,b}\boldsymbol{b}$ and by adopting the notation $[\![\nabla \boldsymbol{u}]\!]\cdot\boldsymbol{\theta}=\frac{\partial[\![u]\!]_n}{\partial\theta}\boldsymbol{n}+\frac{\partial[\![u]\!]_t}{\partial\theta}\boldsymbol{t}+\frac{\partial[\![u]\!]_b}{\partial\theta}\boldsymbol{b}$, the factors of intensity of the constraints equivalents can be written:

$$K_{I,eq}^2=-\frac{E}{1-\nu^2}\int_\Gamma \frac{\partial[\![u]\!]_n}{\partial\theta}t_{c,n}\,d\Gamma$$

$$K_{II,eq}^2=-\frac{E}{1-\nu^2}\int_\Gamma \frac{\partial[\![u_t]\!]}{\partial\theta}t_{c,t}\,d\Gamma$$

$$K_{III,eq}^2=-2\mu\int_\Gamma \frac{\partial[\![u_b]\!]}{\partial\theta}t_{c,b}\,d\Gamma$$

Physically, these expressions quantify the expression of the energy dissipated according to each of the three modes of rupture, if one makes the assumption of a homothetic propagation, in the direction $\boldsymbol{\theta}$, and *that the size of the cohesive zone remains small compared to that of the sample*.

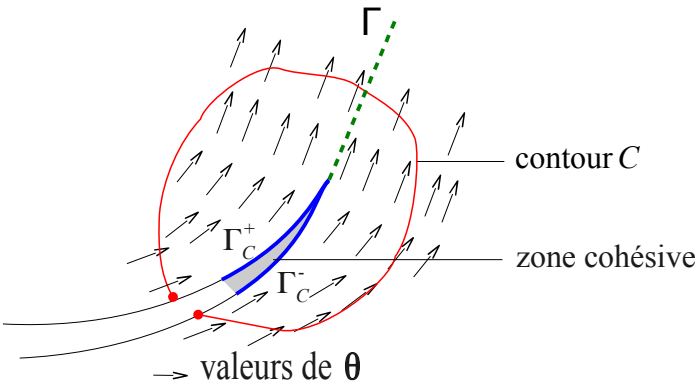

Figure 6.4-a: Definitions of invariant integrals in the presence of a cohesive zone.

The criterion then adopted is the criterion of maximum circumferential constraint of Erdogan and Sih [bib12] (see also [R7.02.13], §2.1):

$$\beta=2\arctan\left[\frac{1}{4}\left(K_I^{èq}/K_{II}^{èq}-sign\left(K_{II}^{èq}\right)\sqrt{\left(K_I^{èq}/K_{II}^{èq}\right)^2+8}\right)\right]$$

Notice – correction of the field θ to make it tangent on the fissured surface:

In order to ensure $\theta\cdot\nabla\varphi_n=0$ in any point M surface fissured (see figures 6.4-b and 6.4-c), the field $\boldsymbol{\theta}$ is corrected in the following way (see fig.6.4-b):

- Initialization $\theta\leftarrow\nabla\varphi_t$;

- Vector θ normal with the plan of propagation: $\boldsymbol{b}\leftarrow\nabla\varphi_n\times\nabla\varphi_t$, then $\boldsymbol{b}\leftarrow\boldsymbol{b}/\|\boldsymbol{b}\|$;

- Correction to ensure θ tangent on the surface of crack: $\theta=\nabla\varphi_n\times\boldsymbol{b}$, then $\theta\leftarrow\theta/\|\theta\|$.

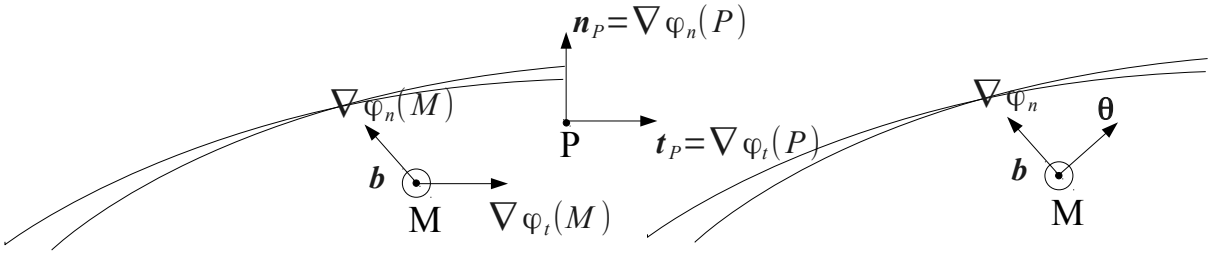

Figure 6.4-b: Correction of the field θ to make it tangent on the fissured surface.

Notice – field θ at the end of the face:

In a method (G,θ) classic, a correction is applied to the values of θ on free surfaces, to ensure $\theta \cdot \nu = 0$, where ν is the normal at free surface (see fig.6.4-c), this in order to avoid negative values of G. This correction is not applied any more in the case of a cohesive calculation (see fig.6.4-c), because this risk is excluded because of nature from calculation (of the surface integrals of dissipation).

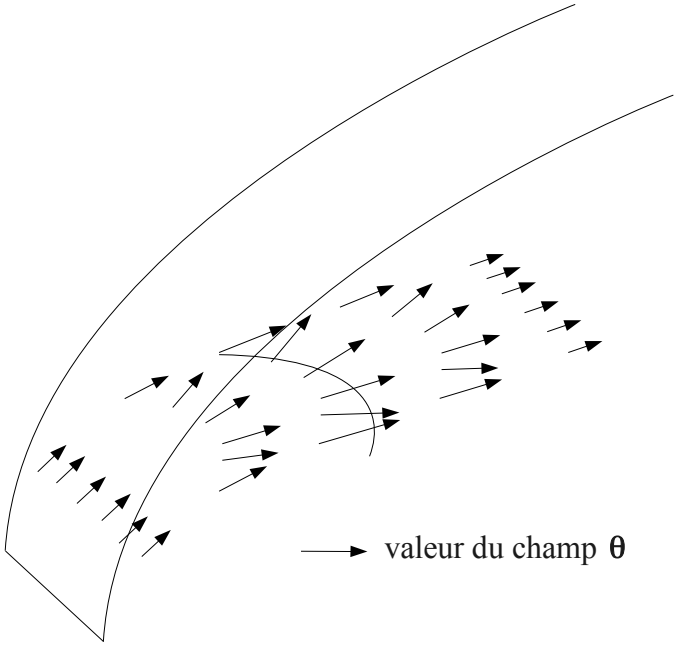

Field θ for a method (G,θ) classic

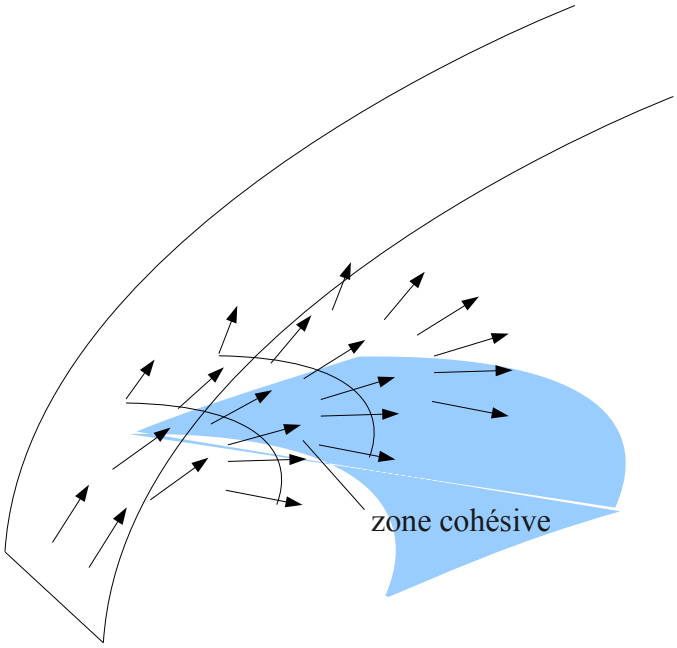

Field θ for a cohesive calculation

Figure 6.4-c: Field θ on the surface fissured for a calculation (G, θ) classical, and for a cohesive calculation.

Notice – choice of the base θ for the decomposition of the modes:

If the cohesive zone has an important size, it is distributed on a curved surface. The choice of the base for the decomposition of the modes is then not obvious: one can choose:
- with the face of crack (figure is the base 6.4-d, solution a),
- is the base at the point considered (fig.6.4-d, solution b),
- is the base related to the polar coordinates with the face of crack (fig.6.4-d, solution c).

While the first solution underestimates the angle of junction and the second over-estimates it, the third solution c) is that which produces the most balanced results, and thus that which was implemented. The calculation of the base thus proceeds as follows:

-Vector position in the reference mark in bottom of crack: $\boldsymbol{PM}=\boldsymbol{x}(M)-\boldsymbol{x}(P)$;

- Projection in the plan: $\boldsymbol{t}\leftarrow\boldsymbol{PM}-(\boldsymbol{PM}\cdot\boldsymbol{b})\boldsymbol{b}$ *, then* $\boldsymbol{t}\leftarrow\boldsymbol{t}/\|\boldsymbol{t}\|$;

- Construction of a vector $\boldsymbol{n}$ *normal:* $\boldsymbol{n}\leftarrow\boldsymbol{t}\times\boldsymbol{b}$ *, then* $\boldsymbol{n}\leftarrow\boldsymbol{n}/\|\boldsymbol{n}\|$.

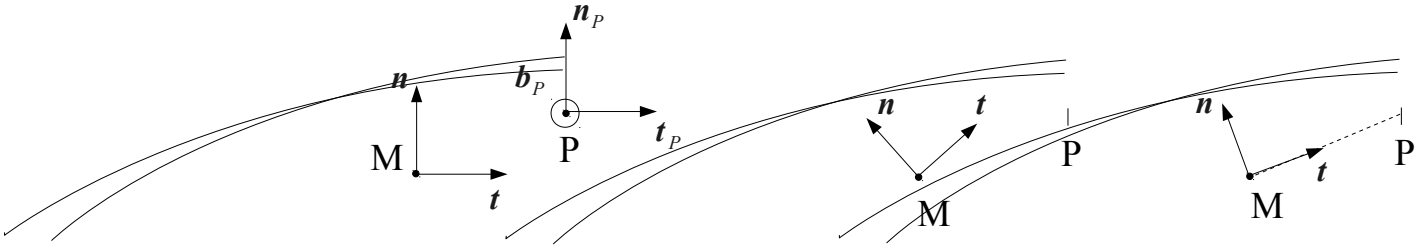

a. base cohesive face b. base covariante local c. base polar coordinates with the cohesive face

Figure 6.4-d: Possible choices of bases for the decomposition of the modes.

6.5 Extension of the potential surface of cracking

For the actualization of fissured surface, we use the algorithm ‘GEOMETRICAL‘described in [R7.02.13], §6. In the phase of detection described in §6.3, only the level-set tangent is brought up to date (OPERATION= 'DETECT_COHESIF‘in PROPA_FISS). In the phase of extension of the potential surface of cracking detailed here (OPERATION= 'PROPA_COHESIF‘in PROPA_FISS), the level-set normal is also brought up to date, and the extension is done according to a fixed length DA_MAX, which must be selected much higher than Δl .

The various methods of actualization of level-sets are indexed in documentation [R7.02.13]. While the classical methods are based on a discretization by centered differences in equations of Hamilton-Jacobi (METHODE_PROPA= 'SIMPLEX‘/’UPWIND‘in PROPA_FISS), simpler methods appeared since (METHODE_PROPA= 'GEOMETRICAL‘in PROPA_FISS), for which the only remaining stage is the update itself. This technique benefits owing to the fact that the surface of crack created at the previous moment is fixed: the problem of propagation of a surface is thus reduced to the propagation of a face from which distances can be directly evaluated.

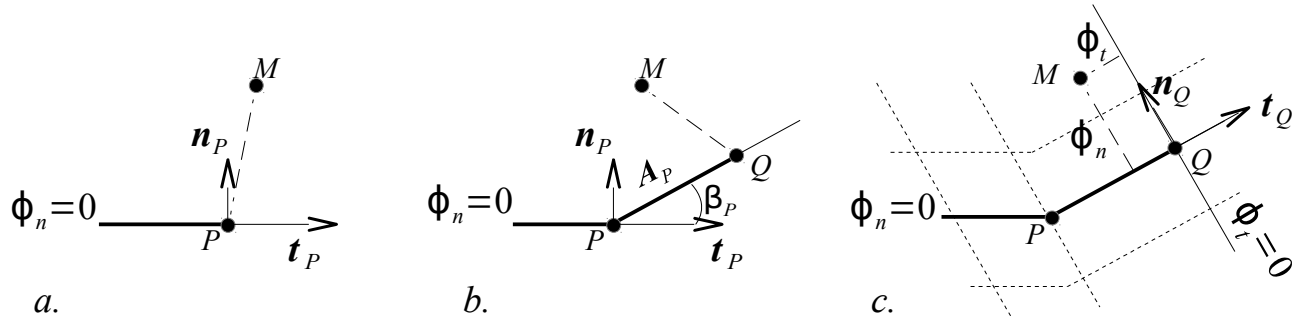

a. *b.* *c.*

Figure 6.5-a: Direct calculation, plan by plan, of new the level-sets by the geometrical algorithm of propagation.

From the equations of evolutions, one manages to show that for each node M , *for little which one manages to project* M *on a point* P *face such as* $M \in (P, \boldsymbol{n}_P, \boldsymbol{t}_P)$, the update is brought back to a problem in this plan $(P, \boldsymbol{t}_P, \boldsymbol{n}_P)$. One thus calculates the new values, *plan by plan*, by plane translations and rotations, as follows:

For each point M of the grid relative:
- One projects this point on the old bottom of crack (fig.6.5-a, stage a).
- One from of deduced projection on the new face (fig.6.5-a, stage b).
- One calculates the level-sets corresponding. If one had $\phi_t(M) \leq 0$, one does not modify $\phi_n(M) \leq 0$, in order to "freeze" existing fissured surface (fig. 6.5-a , stage c).

Notice – correction of the base $(\boldsymbol{n}_p, \boldsymbol{t}_p)$ at the points ends of the face:

An important assumption of the method of propagation geometrical is that the point M *belongs to the plan* $(P, \boldsymbol{n}_p, \boldsymbol{t}_p)$ *(for recall,* M *is the point of the space in which one seeks to bring up to date the level-sets, and* P *is its projection on the bottom of crack). If it is not the case, the base should be corrected* $(\boldsymbol{n}_p, \boldsymbol{t}_p)$ *to ensure this property before applying the algorithm of propagation.*

There are three cases for which this property is not checked, which has the fact in common that the point M *projects itself on an end of the bottom of crack. By* ***chronological order*** *of treatment:*

1. The case of a curved face of crack

In this case, it is necessary to replace $\boldsymbol{t}_P$ *by one* $\boldsymbol{t}'_P$ *tangent at the edge of the structure:* $\boldsymbol{t}'_P \cdot \boldsymbol{\nu} = 0$ *where* $\boldsymbol{\nu}$ *is the normal at the edge of the structure.*

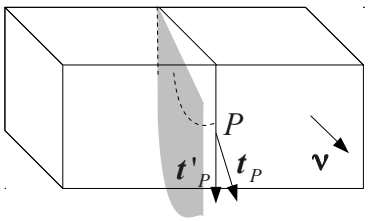

Figure 6.5-b: Case of a curved face of crack.

We will consider that $\boldsymbol{t}_P$ *was corrected according to this procedure thereafter:* $\boldsymbol{t}'_P$ *will be simply noted* $\boldsymbol{t}_P$ *.*

2. The case of a surface fissured tilted compared to the edge of the structure

In this case, it is necessary to correct $\boldsymbol{n}_P$ *by one* $\boldsymbol{n}_P^*$ *, so that* $M \in (P, \boldsymbol{n}_P^*, \boldsymbol{t}_P)$ *. It is not necessary to correct* $\boldsymbol{t}_P$ *. This correction is written:*

$\boldsymbol{n}_P^* \leftarrow (\mathbf{1} - \boldsymbol{t}_P \otimes \boldsymbol{t}_P) \cdot \boldsymbol{PM}$ *, and* $\boldsymbol{n}_P^* \leftarrow \dfrac{\boldsymbol{n}_P^*}{\|\boldsymbol{n}_P^*\|}$.

For a crack which would emerge perpendicularly, one finds well $\boldsymbol{n}_P^* = \boldsymbol{n}_P$.

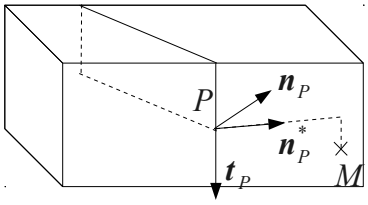

Figure 6.5-c: Case of a surface inclined compared to the edge of the structure.

We will consider that n_P was corrected according to this procedure thereafter: n_P^* will be simply noted n_P .

3. The case of a concave edge of structure

In this case, it is necessary to correct t_P by one t_P^*, so that $M \in (P, n_P, t_P^*)$. It is not necessary to correct n_P . This correction is written:

$t_P^* \leftarrow (1 - n_P \otimes n_P) \cdot PM$, and $t_P^* \leftarrow \frac{t_P^*}{\|t_P^*\|}$

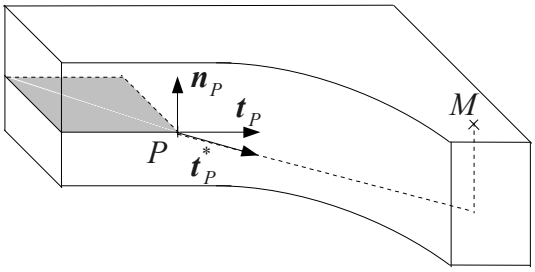

Figure 6.5-d: Case of a concave edge of structure.

6.6 Extension of the space of multipliers and initial internal variables

As illustrated by the figure 6.6-a, stages a-b, the actualization of fissured surface implies that the latter turned upstream of the face. Consequently, the edges which are intersected by the new fissured surface are not the same ones as those which were it by the old one, in particular upstream it face (see fig.6.6-a, stages a-b).

On the fig.6.6-a, stage D, we note Q the whole of the edges intersected by *news* fissured surface, V subset of edges vital (edges which carries a relation of equality), and K the whole of the nodes nouveau riches. We note Q_0, V_0 and K_0 these various units if fissured surface *the preceding one* (fig. is considered.6.6-a, stage a). The whole of vital edges V – which defines the new reduced space of multipliers M_h – is not a subset of Q_0 but of Q .

A reconstruction of V on the basis of zero will probably lead to groups of vital edges very different. As the internal variables are defined on space M_h precedent, they should be projected between two rather different spaces, which would bring a less good conservation of energy. It is thus preferable to build new space by respecting them existing combinations in on this side face, and to

extend it by new groups only in the zone not intersected before, located beyond the face of crack (see fig.6.6-a, stages ac).

One initializes the whole of edges given to the algorithm of restriction on the unit Q edges intersected by *news* fissured surface. Then, one removes this unit (see fig.6.6-a, stage b) edges of $Q_0 \backslash V_0$ of which ends n are both such as:

– for any edge $v \in V_0$ of which n is an end, $v \in Q$.

The algorithm of selection of the vital edges detailed in documentation [R5.03.54, §6] is then implemented: by construction, it will produce a unit V who preserves the groups of preceding nodes (see fig.6.6-a, stage c).

New reduced space implies nodes in $K \backslash K_0$ who did not have values allotted for the internal variables (circle vacuums on the fig.6.6-a, stage c). For such a node n, the initial value is given as follows (see fig.6.6-a, stages Cd):

- If there exists an edge of V connecting n with a node $m \in K_0$, the value of m is allotted to n.
- If not, the initial internal variable is put at 0 (healthy material).

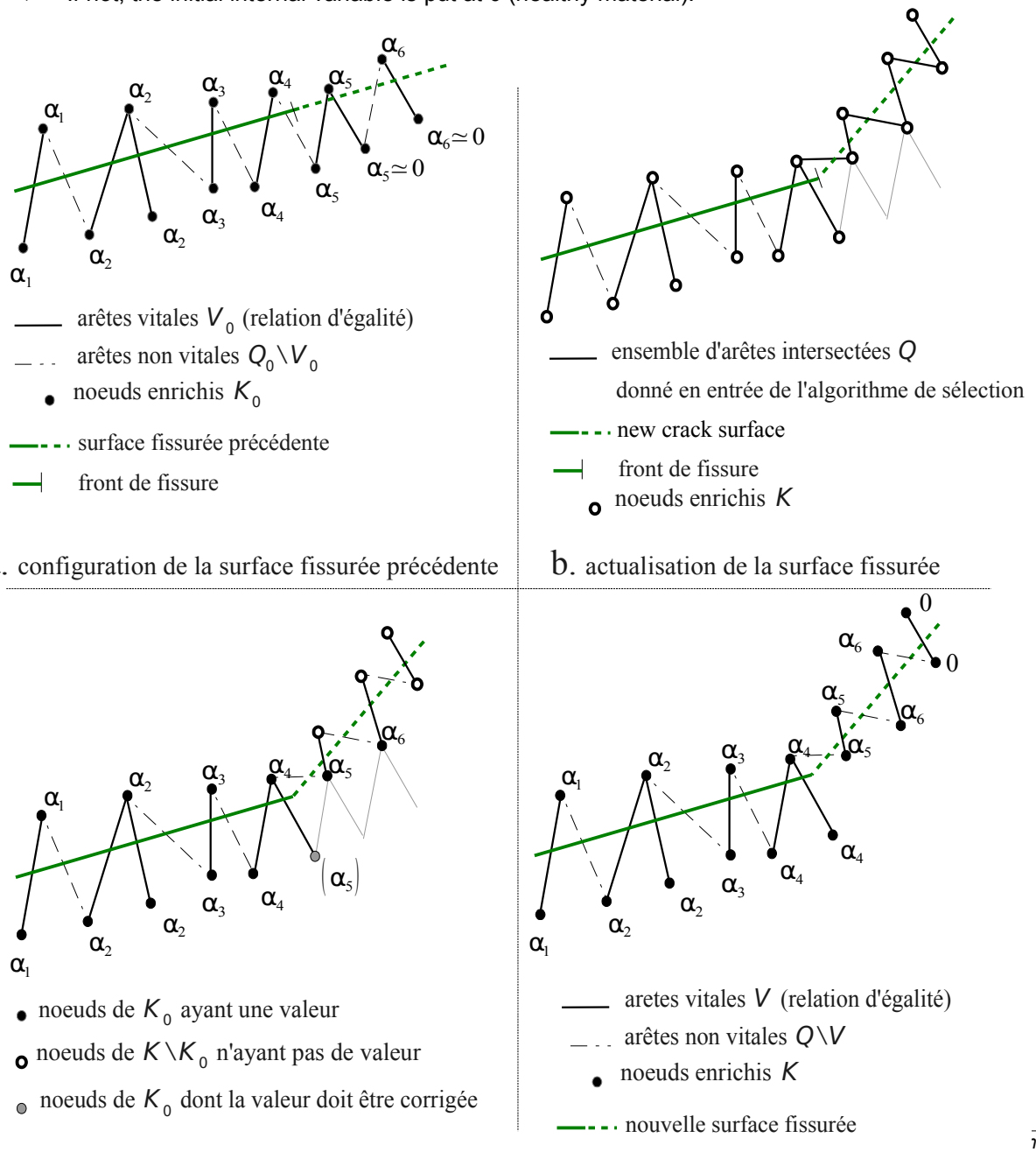

Figure 6.6-a: Extension of the space of multipliers and initial internal variables.

There are also some nodes of K_0 whose value must be changed, because they cont connected to a different group enters V and V_0 (gray circles on the fig.6.6-a, stage c). Once more, if there exists an edge connecting it to a node $m \in K_0$, the value of m is allotted to n. Let us note that the presence of values of not-worthless internal variables although low upstream of the face (such as α_5 and α_6 on the figure 6.6-a, stage a) comes owing to the fact that the face of propagation was smoothed during its detection (see §6.3).

7 Bibliography

1 A. GRIFFITH, “The phenomenon of rupture and flow in solids”, philosophical transactions of the royal society, A221, pp. 98-163, 1920

2 MOËS NR., DOLBOW J., BELYTSCHKO T., “with finite element method for ace growth without remeshing”, International Newspaper for Numerical Methods in Engineering, vol. 46, pp. 135-150, 1999

3 JI H., DOLBOW J.E., “One strategies for enforcing interfacial constraints and evaluating jumps conditions with the extended finite element method”, International Newspaper for Numerical Methods in Engineering, vol. 61, pp. 2508-2535, 2004

4 BOCCA P., CARPITIERI A., VALENTE S. “Mixed mode fractures of concrete”, International Newspaper of Solids and Structures, vol. 27, pp. 1139-1153, 1991

5 CENDON D., GALVEZ J., ELICES MR., PLANED J. “Modelling the concrete fracture of under mixed loading”, International Newspaper of Fracture, vol. 103, pp. 293-310, 2000

6 MESCHKE G., DUMSTORFF P., FLEMING W., JOX S. Computational concrete failure analysis of structures using the extended finite element method. Neue Bauweisen, trends in Statik und Dynamik, 2.395 – 408.2006.

7 ZAMANI A., REPRIEVES R., Cohesive ESLAMI Mr. “and not-cohesive fracture by higher order enrichment of XFEM”. Int. J. Num. Meth. Engng, 90.452 – 483.2012.

8 MOËS NR., BELYTSCHKO T. “Extended finite element method for cohesive ace growth”. Engineering fractures mechanics, 69.813 – 833.2002.

9 ELICES MR., PLANED J. “Asymptotic analysis of has cohesive ace: 1.theoretical background”. International Newspaper of Fracture , 55.153 – 177.1992.

10 MESCHKE G., DUMSTORFF cohesive P. Energy-based modelling of and cohesionless aces via X-FEM. Computational Methods in Applied Mechanics Engineering, 196.2338 – 2557.2007.

11 FRIES T.P., BAYDOUN Mr. Crack propagation with the extended finite element method and has hybrid explicit-implicit ace description. International Newspaper for Numerical Methods in Engineering, 89.1527 – 1558.2012.

12 ERDOGAN F., SIH G.C. One the ace entension in plane loading and transverse shear. Newspaper BASIC Engng, 85.519 – 527.1963.

8 Description of the versions

Index document	Version Aster	Author (S) Organization (S)	Description of the modifications
With	12	G. FERTE, P.MASSIN EDF/R & D AMA	Initial text